Thermal performance of hybrid nanofluid in a rotating vertical channel between two plates

Thesis Submitted By

ROBASH QASIM

(01-248192-006)

Supervised By

Dr. Rizwan ul Haq

Department of computer science

Bahria University, Islamabad

Session (2019-2021)

Thermal performance of hybrid nanofluid in a rotating vertical channel between two plates

Thesis Submitted By

ROBASH QASIM

(01-248192-006)

Supervised By

Dr. Rizwan ul Haq

A Dissertation submitted to the Department of Computer Sciences, Bahria University, Islamabad as a partial fulfillment of the requirements for the award of the degree of MS (Mathematics)

Session (2019-2021)

Bahria University
Discovering Knowledge

MS-13

Thesis Completion Certificate

Students Name: **Robash Qasim** Registration Number: **66195**

Program of study: **MS (Mathematics)**

Thesis Title: **"Thermal performance of hybrid nanofluid in a rotating vertical channel between two plates"**

It is to certify that the above student's thesis has been completed to my satisfaction and to my belief, its standard is appropriate for submission for Evaluation. I have also conducted plagiarism test of this thesis using HEC prescribed software and found similarity index at 17% that is within the permissible limit set by HEC for MS/MPhil degree thesis. I have also found the thesis in a format recognized by the BU for MS/MPhil thesis.

Principal Supervisor's signature: _____

Name: **Dr. Rizwan ul Haq** Date: 20-09-2021

Bahria University
Discovering Knowledge

MS-14A

Author's Declaration

I, **Robash Qasim** here by state that my MS thesis Title **"Thermal performance of hybrid nanofluid floe in a rotating vertical channel between two plates"** is my own work and has not been submitted previously by me for taking any degree from Bahria University or anywhere else in the country/world.

At any time if my statement is found to be incorrect even after my postgraduate, the university has the right to withdraw/cancel my MS degree.

Name of student: **Robash Qasim**

Date: __20-09-2021

Bahria University
Discovering Knowledge

MS-14B

Plagiarism Undertaking

I, **Robash Qasim** solemnly declare that research work presented in the thesis titled **"Thermal performance of hybrid nanofluid in a rotating vertical channel between two plates"** solely my research work with no significant contribution from any other person. Small contribution/help wherever taken has been duly acknowledge and that complete thesis has been written by me.

I understand the zero-tolerance policy of the HEC and Bahria University towards plagiarism. Therefore, I as an author of the above title thesis declare that no portion of my thesis has been plagiarized and any material used as reference is properly referred/cited.

I undertake that if I am found guilty of any formal plagiarism in the above titled thesis even after award of MS degree, the university reserves the right to withdraw/revoke my MS degree and that HEC and the University has the right to publish my name on the HEC/University website on which names of students are placed who submitted plagiarized thesis.

Author's sign: _______

Name of the Student: **Robash Qasim**

Dedicated to

My beloved parents and respected teachers

Thanks for your love, pray and support.

My supporting brother and caring sisters

Thanks for all your love to me

Acknowledgments

Praise to be **Almighty Allah**, who is the Lord of the world, the Answer of prayers and the source of peace, whose blessing and exaltation flourished to the scared wealth of knowledge. Indeed, this difficult task was made possible with the help of **Allah**. Special praise and regards for his Last messenger, Holy Prophet **Hazrat Muhammad (PBUH).** Holy Prophet said that I AM the light, whoever follows ME, will never be in the darkness.

I feel great pleasure in expressing my profound and heartiest gratitude to my kind, devoted supervisor **Dr. Rizwan ul Haq**, for his indispensable guidance, deep consideration, affection and active co-operation that made possible to this work to meet its end successfully well in time. Teachers like him are very precious assets for a nation who change the life of an individual and also nations. Such teachers make the density of a nation. I am proud that my supervisor is also one of the teachers and working with him is an honor for me.

I would also express my gratitude to all teachers. Due to their guidance and help am able to get the success of reaching my destination. The prominent among them are **Dr. Muhammad Ramzan** and **Dr. Jafar Husnain** who supported me in all course work as well as in the completion of this thesis. I like to thanks to all respected teachers at Department of Mathematics, Bahria University Islamabad Campus for providing us healthy academic environment.

I express my gratitude to my family member who provided me every moral and financial during my study at Bahria University and thus I was able to accomplish core task of thesis, without their continuous help i could not imagine to achieve this goal. I am also thankful to my friends who provided me every assistance during my study, Tabinda sajjad, Ali Raza, and Syed Saqib Ali shah. At the end I would acknowledge the pleasant moments with my all fellows.

Robash Qasim

Bahria University, Islamabad

Abstract

The main purpose of this thesis is construct the mathematical model of the fluid flow in a rotating system between two infinitely flat surfaces. In this model one plate is stretchable while other is penetrable. By using basic fundamental law, equation of momentum and energy are formulated. Then, these energy and momentum equations are converted in to non-linear ordinary differential equation by using similarity variables. Theses ordinary differential equation are further solve by using Adomian decomposition method (ADM). The impact of various parameters on temperature and velocity profiles are investigate. The obtained result shows the variation of Nusselt number by increasing the radiation and injection parameter. This thesis is split in to five chapter. In chapter 1 comprehensive review analysis is done to determine gape exist, where we can fill up by developing the modification in fundamental laws and methodology. Chapter 2 is related to basic concept of fluid and its properties of fluid. Chapter 3 is review work done by Ali J Chamkha et al [35] that deals flow of hybrid nanofluid between two parallel plates. Chapter 4 is the extension of chapter 3 in which we have developed the channel flow with various effects that improve the thermal conductivity and flow behavior between the channels. In the very last chapter, conclusion of entire analysis is presented.

Contents

Acknowledgments

Nomenclature

Abstract

1 Introduction and literature Review 1

2 Elementary concepts 4

2.1 Fluid Mechanics 4

2.2 Fluid 4

2.2.1 **Some important fluid properties** 4

2.2.2 Pressure 4

2.2.3 Density 4

2.2.4 Viscosity 4

2.3. Kinds of fluid 4

2.3.1 Ideal fluid 4

2.3.2 Real fluid 5

2.3.3 Steady 5

2.3.4 Unsteady 5

2.3.5 Compressible 5

2.3.6 Incompressible 5

2.3.7 Rotational 5

2.3.8 Irrotational flow 5

2.3.9 One dimensional flow 5

2.3.10 Two dimensional flow 5

2.3.11 Three dimensional flow 5

2.3.12 Heat transfer 5

2.3.13 Thermal energy 6

2.3.14 Magnetohydrodynamic (MHD) 6

2.3.15 Thermal conductivity 6

2.3.16 Nanofluid 6

3. Magneto-hydrodynamic flow and heat transfer of a hybrid nanofluid in a rotating system between two surfaces in the presence of thermal radiation and Joule heating 7

3.1 Formulation and solution 7

3.2 Analytical method 12

3.3 Result and discussion 17

4. Thermal performance of hybrid nanofluid in a rotating vertical channel 29

4.1 Modeling of problem 30

4.2 Methodology 33

4.3 Result and discussion 34

5. Conclusion 48

Bibliography 49

References

List of Figures

3.1. Geometry of problem. 7

3.2. Variations of suction\injection parameter with respect to velocity profile $f(\eta)$in *x*-direction. 19

3.3. Variations of suction\injection parameter with respect to velocity profile $g(\eta)$ in *z*-direction. 19

3.4. Influence of Reynolds number with respect to velocity profile $f(\eta)$ in *x*-direction. 20

3.5. Influence of Reynolds number with respect to velocity profile $g(\eta)$ in *y*-direction. 20

3.6. Influence of suction\injection parameter on temperature θ . 21

3.7. Variation of Reynolds number with temperature profile θ . 21

3.8. Impact of suction\injection parameter and Reynolds number on Nusselt number. . 22

3.9. Magnetic field variations with velocity profile $f(\eta)$ in *x*-direction. 23

3.10. Magnetic field variations with velocity profile $g(\eta)$ in *z*-direction. 23

3.11. Rotational effects with velocity profile $f(\eta)$ in *x*-direction. 24

3.12. Rotational effects with velocity profile $g(\eta)$ in *z*-direction. 24

3.13. Influence of magnetic parameter on temperature profile θ . 25

3.14. Variation of Rotation parameter with temperature profile θ . 25

3.15. Impact of magnetic parameter and Rotational parameter on Nusselt number. 26

3.16. Variation of *N* on temperature profile θ . 27

3.17. Variation of volume fraction on temperature profile θ . 27

3.18. Impact of volume fraction and *N* on Nusselt number. 28

4.1 Geometry of problem. 29

4.2. Variations of suction\injection parameter and Reynolds number with respect

To velocity profile $f(\eta)$ in *x*-direction. 36

4.2. Variations of suction\injection parameter and Reynolds number with respect to

Velocity profile $g(\eta)$ in *z*-direction. 36

4.3. Variations of suction\injection and Reynolds number with respect

To temperature profile θ . 38

4.4. Impact of suction\injection and Reynolds number on Nusselt

Number. 40

4.5. Influence of magnetic parameter and rotation parameter on temperature

Profile θ . 42

4.6. Variation of N and volume fraction on temperature profile. 45

4.7. Variations of Grashaf number with respect to temperature profile θ and velocity

Profile in *x* and *z*-direction. 47

List of Tables

1. Thermal properties of Go andCu. 12

2. Comparison of results of Nusselt number. 17

Nomenclature

u^*, v^*, w^*	Velocity components
T^*	Temperature
P	Pressure
$\bar{\sigma}$	Electrical conductivity
σ^*	Stefan Boltzmann constant
g	Magnitude of acceleration due to gravity
ρ_{hnf}	Hybrid nanofluid effective density
μ_{hnf}	Hybrid nanofluid f dynamic viscosity
μ_f	Base fluid's dynamic viscosity
k_{hnf}	Hybrid nanofluid thermal conductivity
k^*_{hnf}	Hybrid nanofluid's mean absorption coefficient
k_f	Base fluid's thermal conductivity
ρ_f	Base fluid's viscosity
ν_f	Kinematic viscosity
$(\rho C_p)_{hnf}$	Hybrid nanofluid heat capacity
$(\rho C_p)_f$	Base fluid's heat capacity
β	Thermal expansion coefficient
Mn	Magnetic parameter
N	Radiation parameter
Ro	Rotation parameter
Re	Reynold number
A	Suction/injection
Ec	Eckert number
Pr	Prandtl number
Gr_m	Mixed convection parameter
Q_o	Heat generation/absorption
Q	Heat source or sink parameter
Gr	Grashaf number
MHD	magneto-hydrodynamic

Chapter1

1. Introduction and literature review

Heat transfer and rotating flow study has huge scope due to its large application in many industries like transportation and engineering. Such techniques are helpful in heat transfer enhancement and nanofluid plays a vital role in heat transfer. The term nanofluid can be expressed as suspension of nanometer sized particle with some base fluid. Water and other lubricant are used as base fluid. Nanoparticles like *Al, Ag* and *Cu* are used for the production of nanofluid. Nanofluid was first ever proposed by *Choi.* [1]. He used nanoparticles to increase the thermal conductivity of base fluid. These tiny size particles are mostly of metals, oxide and carbides. Nanofluids are commonly used in many fields like Medical and pharmacy. Due to enormous application nanofluid receives special attention from several bright researchers. Das. [2] also examined the flow behavior of nanofluid with alumination. Number of authors [3-10] explained the vital relationship between heat transfer and nanofluid particles.

Magnetohydrodynamic (MHD) is the combination of words magneto-meaning magnetic, hydro-meaning fluid and dynamic- meaning movement. It is the phenomena in which fluid is electrically conducting in the presence of magnetic field. In 1942, Swedish scientist Hannes Alfven et al. [11] introduced the term MHD in his paper and discovered the MHD waves known as Alfven, Which has number of application in astrophysical problems. MHD flow between two parallel plates has importance in many applications such as; MHD generator, pumps, cooling of nuclear reactor. The experimental investigation on MHD flow was carried out by Hartman and Lazarus et al. [12] and they analyzed the influence of effects of uniform magnetic field on the flow of electrically conducting fluid between parallel plates. Later on, Rosson et al. [13] also investigated the flow of electrically conducting fluid over flat plate in the presence of magnetic field. The investigation also found that fluid velocity changes due to this magnetic field.

As nanoparticles in fluid raise the thermal conductivity [1], they are used in magneto hydrodynamic (MHD) flow along with radiation to accumulate its efficiency. Effect of MHD is used by many renowned researchers due to its characteristic of heat transfer. Heat transfer is a process of exchanging thermal energy which takes place through conduction, convection and radiation. Research studies confirm that the heat transformation of nanofluid in rotating surfaces between two parallel plates. According to the Mustafa et al. [14] heat transfer enhancement

significantly depends upon nano-sized particles. The study also found that Nusselt number is increasing function of Prandtl number. Another study made by Alizdin et al. [15] regarding the magneto hydrodynamic micro-polar fluid with in a channel filled with nanofluid under the influence of thermal radiation. Results show that by increasing radiation parameter and volume fraction, Nusselt number also increases. Ellahi et al. [16] studied the flow in a pipe with MHD effects at nanofluid. It was observed that MHD parameters reduce the motion of fluid and when variable viscosities occur velocity is greater than the temperature. Another study on heat transfer between two surfaces and rotating channel was published by Sheikholeslami et al. [17]. The study discussed that the surface heat transfer rate increases the suction/injection parameter and nanofluid volume fraction. The impact of nano-particle magneto hydrodynamic flow in a rotating channel under influence of thermal radiation is explained by some researchers [18-31].

The nonlinear movement of nanoparticles in the fluid is Brownian motion which is obtained from the motion of the molecules of fluid. The nonlinear motion of fluid is due to the position of nanoparticle within the sub-domain of fluid. Thermal equilibrium of fluid is defined by this motion through its temperature. Fluid also remain linear all time because of the Brownian motion. After the botanist Robert Brown, this motion of nanoparticle is named as Brownian motion. In 1905, Albert Einstein defined this Brownian movement in his paper and his paper has made a huge contribution in science.

Currently, researcher use another kind of nanofluid called hybrid nanofluid that is formed by using two or more different material of nanofluid. Hybrid nanofluid is used for further improvement of heat and mass transfer among the surfaces. Chamkha et al. [32] used hybrid nanofluid in their experiment and results show that by using hybrid nanofluid the average Nusselt number increases. Glora et al. [33] also studied the impact of hybrid nanofluid flow in a square porous with heat source/sink. Their study shows that Nusselt number decrease by changing the position of heat source. Further, they explore that as compared to nanofluid, hybrid nanofluid has low average Nusselt number. Tayebi and Chamkha. [34] Proved by their experiments that by using hybrid nanofluid heat transfer rate become more efficient. Recently, analytical technique is introduced to solve the nonlinear problems. Liao et al. [35] introduce this technique in his problem. Results shows that analytical technique has successfully been applied to many nonlinear problems.

Flow in a channel is one of the most significant branch of fluid mechanics where fluid is enclosed between two surfaces no matter both the surfaces are flat or corrugated. Channel is further discuss in two ways i.e., open channel and closed channel. In open channel flow is depending upon

time. Viscosity and inertia have strong effect on open channel flow. Flow that occurs in a closed contaminant is closed channel flow. In closed channel flow is either Laminar or Turbulent. In Laminar flow velocity of every particle remain constant and during flow layers do not intersect with each other while flow of liquid is irregular in turbulent flow.

Based on above mentioned literature review, entire thesis is set up for rotating channel flow filled by hybrid nanofluid. Chapter 3, discusses the review of published work done by Ali J Chamkha et al [35]. In chapter 4, I have extended the chapter 3 for new effects as: Mixed convection and heat generation/absorption in vertical rotating channel and stretchable surface. Finally, chapter 5 addresses the thorough conclusion of this thesis.

Chapter 2

Elementary concepts of fluid

In this section some essential definition are discussed.

2.1. Fluid mechanics

Branch of mechanics that deals with fluid behavior at rest and motion.

2.2. Fluid

Substance that continuously deform when pressure is applied is called fluid. For example blood, air, honey.

2.2.1. Physical properties

Some fundamental properties are defined below.

2.2.2. Pressure

The force which applied perpendicularly to the surface and cause some effects called pressure. Mathematical form of pressure is;

$$P = \frac{force}{area} = \frac{F}{A}$$

2.2.3. Density

When mass is divided by volume of fluid particle it gives density of that object .it is denoted by "ρ" and defined as;

$$\rho = \frac{mass}{volume}$$

2.2.4. Viscosity

Force which resistance the motion of fluid is known as viscosity. Mathematical form is "μ".

$$\mu = \frac{shear\ stress}{rate\ of\ deformation}$$

2.3. Kinds of fluid

2.3.1. Ideal fluid

Fluid which has zero viscosity is ideal fluid.

2.3.2. Real fluid

Fluid that contains viscosity or viscous force is called real fluid. For example, air, honey etc.

2.3.3. Steady flow

Flow that is not time dependent is steady flow. Mathematical form is;

$$\frac{\partial \eta}{\partial t} = 0$$

2.3.4. Unsteady flow

Flow that is time dependent is unsteady flow.

2.3.5. Compressible flow

Flow in which density changes due to stress called compressible flow. For example gases etc.

2.3.6. Incompressible flow

Flow in which density does not change is consider as incompressible flow. Liquids and lubricants are usually incompressible.

2.3.7. Rotational flow

Flow in which fluid particle rotate with some angular velocity is rotational flow.

$$\frac{\partial \eta}{\partial t} = 0$$

2.3.8. Irrotational flow

Flow in which fluid particles does not rotate is irrotational flow.

2.3.9. One dimensional flow

Flow which depends on one co-ordinate and all particles are parallel to certain straight line is known as one dimensional flow.

2.3.10. Two dimensional flow

Flow which depends on two co-ordinates and velocity is parallel to plane is known as two dimensional flow.

2.3.11. Three dimensional flow

Fluid flow which depends on all co-ordinates of space is known as three dimensional flow.

2.3.12. Heat transfer

The phenomena in which heat is transfer from one location to another with the motion of molecule.

2.3.13. Thermal energy

Internal energy kept by a system or objects because of the movement of molecules is called thermal energy.

2.3.14. Magnetohydrodynamics

The study of electrically conducting fluid in the presence of magnetic field is known as MHD.

2.3.15. Thermal conductivity

The process of heat transfer because of internal capability of any material is thermal conductivity**.**

2.3.16. Nanofluid

Nanofluid is the mixture of nano meter size particles and base fluid. The base fluid may be Newtonians and non-Newtonian. Mathematically we can write it as

$$\lambda = \frac{\alpha}{\delta}$$

Chapter 3

Magneto-hydrodynamic flow and heat transfer of a hybrid nanofluid in a rotating system between two surfaces in the presence of thermal radiation and Joule heating

In this chapter rotating flow of hybrid nanoparticles and heat transfer property is discussed. First we formulate the basic equation of momentum and energy. Resulted PDE's are further transformed in to corresponding ODE's. Then we convert higher order nonlinear ODE's in system of first order equation and applied numerical technique. Result are discussed in detail for each parameter involved in equation.

3.1 Formulation and solution

Consider steady, incompressible flow between two parallel plates. Due to rotation of channel fluid is rotating with velocity Ω. Motion of lower plate is due to velocity $u^* = u_w^* = ax$.

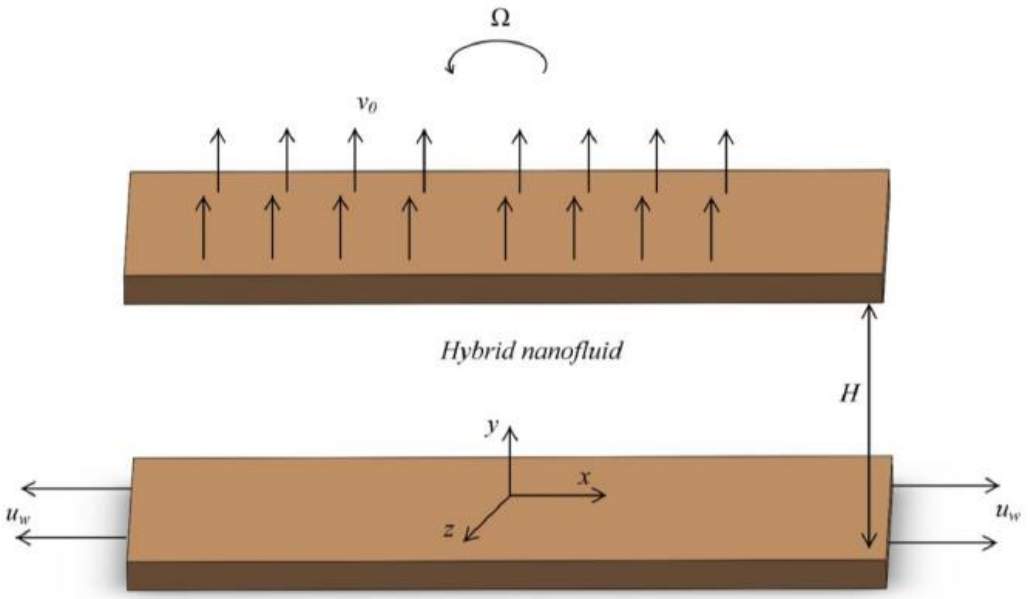

Figure 3.1: Geometry of problem

$$\boldsymbol{\nabla}.\boldsymbol{V} = 0 \tag{3.1}$$

$$\rho_{hnf}\left(\frac{d\boldsymbol{V}}{dt} + 2\Omega \times \mathbf{V} + \Omega \times (\Omega \times \mathrm{r})\right) = \mathrm{div}\tau - \bar{\sigma}_f B_o^2 \boldsymbol{V}, \tag{3.2}$$

$$(\rho C_p)_{hnf}\left((\boldsymbol{V}.\boldsymbol{\nabla})\mathrm{T}^*\right) = \boldsymbol{\tau}.\mathbf{L} - \bar{\sigma}_f B_o^2 \boldsymbol{V}, \tag{3.3}$$

Where V is the velocity in x, y, z direction.

$$\tau = -\ddot{p}I + \mu A_1, \tag{3.4}$$

μ Represent the viscosity and A_1 is Rivlin-Ericksen tensor,

$$A_1 = \boldsymbol{L} + \boldsymbol{L^t}, \tag{3.5}$$

$$\boldsymbol{L} = \boldsymbol{\nabla}.\boldsymbol{V}, \tag{3.6}$$

Temperature and velocity are respectively given as

$$T^* = T^*(x, y, z), \qquad \boldsymbol{V} = [u^*(x, y), v^*(x, y), w^*(x, y)],$$

$$\boldsymbol{L} = \begin{bmatrix} u_x^* & u_y^* & 0 \\ v_x^* & v_y^* & 0 \\ w_x^* & w_y^* & 0 \end{bmatrix} \tag{3.7}$$

Where $u_x^* = \frac{\partial u^*}{\partial x}$, $v_x^* = \frac{\partial v^*}{\partial x}$, $w_x^* = \frac{\partial w^*}{\partial x}$ and $u_y^* = \frac{\partial u^*}{\partial y}$, $v_y^* = \frac{\partial v^*}{\partial y}$, $w_y^* = \frac{\partial w^*}{\partial y}$

$$\boldsymbol{L^t} = \begin{bmatrix} u_x^* & v_x^* & w_x^* \\ u_y^* & v_y^* & w_y^* \\ 0 & 0 & 0 \end{bmatrix} \tag{3.8}$$

By using equations (3.7) and (3.8) in (3.5) we get

$$A_1 = \begin{bmatrix} 2u_x^* & v_x^* + u_y^* & w_x^* \\ u_y^* + v_x^* & 2v_y^* & w_y^* \\ w_x^* & w_y^* & 0 \end{bmatrix} \tag{3.9}$$

By using (3.9) in (3.4) we get

$$\tau = \begin{bmatrix} 2\mu u_x^* - p & \mu(v_x^* + u_y^*) & \mu w_x^* \\ \mu(u_y^* + v_x^*) & 2\mu v_y^* & \mu w_y^* \\ \mu w_x^* & \mu w_y^* & -p \end{bmatrix} \tag{3.10}$$

Momentum equation in reduce form for rotational flow is

$$\rho_{hnf}\frac{\partial \boldsymbol{V}}{\partial t}+2\Omega\times\mathbf{V}=\mathrm{div}\tau+J\times B, \tag{3.11}$$

Where $\Omega=[0,\Omega,0]$ and $J\times B=[-\bar{\sigma}_f B_o^2 u^*,0,-\bar{\sigma}_f B_o^2 w^*]$.

For law of conservation of mass, continuity equation define as:

$$\frac{\partial v^*}{\partial y}+\frac{\partial u^*}{\partial x}=0 \tag{3.12}$$

For the momentum equation

Along x-component:

$$\rho_{hnf}\frac{\partial \boldsymbol{V}}{\partial t}+2\Omega\times\mathbf{V}=\frac{\partial}{\partial x}\,\tau_{xx}+\frac{\partial}{\partial y}\,\tau_{xy}\,, \tag{3.13}$$

By using (3.10) in (3.11) we have

$$v^*\frac{\partial u^*}{\partial y}+u^*\frac{\partial u^*}{\partial x}+2\Omega\mathrm{w}^*=-\frac{1}{\rho_{hnf}}\frac{\partial P}{\partial x}+\frac{\mu_{hnf}}{\rho_{hnf}}\left(\frac{\partial^2 u^*}{\partial x^2}+\frac{\partial^2 u^*}{\partial y^2}\right)-\frac{\bar{\sigma}_f B_o^2}{\rho_{hnf}}u^*. \tag{3.14}$$

Along y -component:

$$\rho_{hnf}\frac{\partial \boldsymbol{V}}{\partial t}+2\Omega\times\mathbf{V}=\frac{\partial}{\partial x}\,\tau_{yx}+\frac{\partial}{\partial y}\,\tau_{yy}\,, \tag{3.15}$$

By using (3.10) in (3.14)

$$v^*\frac{\partial v^*}{\partial y}+u^*\frac{\partial v^*}{\partial x}=-\frac{1}{\rho_{hnf}}\frac{\partial P}{\partial y}+\frac{\mu_{hnf}}{\rho_{hnf}}\left(\frac{\partial^2 v^*}{\partial x^2}+\frac{\partial^2 v^*}{\partial y^2}\right). \tag{3.16}$$

Along z -component:

$$\rho_{hnf}\frac{\partial \boldsymbol{V}}{\partial t}+2\Omega\times\mathbf{V}=\frac{\partial}{\partial x}\,\tau_{zx}+\frac{\partial}{\partial y}\,\tau_{zy}\,, \tag{3.17}$$

By using (3.10) in (3.16) we get

$$v^*\frac{\partial w^*}{\partial y}+u^*\frac{\partial w^*}{\partial x}-2\Omega\mathrm{u}^*=\frac{\mu_{hnf}}{\rho_{hnf}}\left(\frac{\partial^2 w^*}{\partial x^2}+\frac{\partial^2 w^*}{\partial y^2}\right)-\frac{\bar{\sigma}_f B_o^2}{\rho_{hnf}}w^*\,. \tag{3.18}$$

For energy equation, we have:

$$(\rho C_p)_{hnf}\left((\boldsymbol{V}.\boldsymbol{\nabla})\mathrm{T}^*\right)=\boldsymbol{\tau}.\mathbf{L}+J\times B\,, \tag{3.19}$$

Using value of $\boldsymbol{\tau}.\mathbf{L}$ in equation (3.18) we have

$$v^*\frac{\partial T^*}{\partial y}+u^*\frac{\partial T^*}{\partial x} = \frac{k_{hnf}}{(\rho C_p)_{hnf}}\left(\frac{\partial^2 T^*}{\partial x^2}+\frac{\partial^2 T^*}{\partial y^2}\right)-\frac{1}{(\rho C_p)_{hnf}}\frac{\partial q^*_{rad}}{\partial y} + \frac{\bar{\sigma}_f\, B_o^2}{(\rho C_p)_{hnf}}\left(u^{*2}+w^{*2}\right), \tag{3.20}$$

In equations Ω is angular velocity, u^*, w^*, v^* are velocities in x, y and z directions, B_o is mangnetic field, P is pressure, $T^*$is temperature, $\bar{\sigma}_f$ is electrical conductivity and q^*_{rad} is radiative demonstrate heat flux.

For radiation

$$q^*_{rad} = -\left(\frac{4\sigma^*}{3k^*_{hnf}}\right)\frac{\partial T^{*4}}{\partial y}, \tag{3.21}$$

We can expand T^{*4} in a Taylor series and by this expansion we get

$$T^{*4} \cong -3T^{*4}_{\infty}+4T^{*3}_{\infty}T^*, \tag{3.22}$$

So the equation (3.19) become

$$v^*\frac{\partial T^*}{\partial y}+u^*\frac{\partial T^*}{\partial x} = \frac{k_{hnf}}{(\rho C_p)_{hnf}}\left(\frac{\partial^2 T^*}{\partial x^2}+\frac{\partial^2 T^*}{\partial y^2}\right)+\frac{16\sigma^* T^{*3}_{\infty}}{3k^*_{nf}(\rho C_p)_{nf}}\frac{\partial^2 T^*}{\partial y^2} + \frac{\bar{\sigma}_f B_o^2}{(\rho C_p)_{hnf}}\left(u^{*2}+w^{*2}\right), \tag{3.23}$$

Effective dynamic viscosity, heat capacity and thermal conductivity are define as:

$$\rho_{hnf} = (1-\phi_{Cu}-\phi_{Go})\rho_f+\phi_{Cu}\rho_{Cu}+\phi_{Go}\rho_{Go}, \tag{3.24}$$

$$(\rho C_p)_{hnf} = (1-\phi_{Cu}-\phi_{Go})(\rho C_p)_f+\phi_{Cu}(\rho C_p)_{Cu}+\phi_{Go}(\rho C_p)_{Go}, \tag{3.25}$$

$$\mu_{nf} = \mu_f(1-\phi_{Cu}-\phi_{Go})^{-2.5}, \tag{3.26}$$

$$\frac{k_{hnf}}{k_f} = \left\{\frac{k_{Cu}\phi_{Cu} + k_{Go}\phi_{Go}}{\phi_{Cu} + \phi_{Go}} + 2k_f + 2(k_{Cu}\phi_{Cu} + k_{Go}\phi_{Go}) - 2(\phi_{Cu} + \phi_{Go})k_f\right\}\left\{\frac{k_{Cu}\phi_{Cu} + k_{Go}\phi_{Go}}{\phi_{Cu} + \phi_{Go}} + 2k_f - (k_{Cu}\phi_{Cu} + k_{Go}\phi_{Go}) + (\phi_{Cu} + \phi_{Go})k_f\right\}^{-1}. \quad (3.27)$$

Table1. Thermo physical properties of hybrid nanofluid and water.

	(kg/m^3)	**C_p(J/kg K)**	**k(W/m k)**
Graphene Oxide (Go)	1800	717	5000
Copper (Cu)	8933	385	401
Pure water	997.1	4179	0.613

Boundary conditions at lower and upper surfaces are:

$$u^* = u_w^* = ax, \qquad v^* = 0, \quad w^* = 0, \qquad T^* = T_H^* \qquad at\ y = 0 \quad (3.28)$$

$$u^* = 0, \qquad v^* = v_o, \quad w^* = 0, \qquad T^* = T_o^* \qquad at\ y = h \quad (3.29)$$

Using similarity variables:

$$\eta = \frac{y}{h}, \quad v^* = -ahf(\eta), \qquad u^* = axf'(\eta), \quad w^* = axg(\eta), \quad \theta = \frac{T^* - T_H^*}{T_o^* - T_H^*}. \quad (3.30)$$

By using similarity variables the given PDE's transformed in to dimensionless ODE's.

$$f^{iv} + Ƀ_1(1 - \phi_{Cu} - \phi_{Go})^{2.5}Re(ff''' - f'f'') - 2Ƀ_1R_o((1 - \phi_{Cu} - \phi_{Go})^{2.5}g' - Mn((1 - \phi_{Cu} - \phi_{Go})^{2.5}f'' = 0, \quad (3.31)$$

$$g'' + Ƀ_1(1 - \phi_{Cu} - \phi_{Go})^{2.5}Re(fg' - f'g) + 2Ƀ_1R_o((1 - \phi_{Cu} - \phi_{Go})^{2.5}f' - Mn((1 - \phi_{Cu} - \phi_{Go})^{2.5}g = 0, \quad (3.32)$$

$$\theta'' + Ƀ_2PrRe\left(\frac{3}{3 + 4N}\right)\frac{k_f}{k_{hnf}}f\theta' + MnPrEc\left(\frac{3}{3 + 4N}\right)\frac{k_f}{k_{hnf}}(f'^2 + g^2) = 0. \quad (3.33)$$

$Ƀ_1$, $Ƀ_2$ are constant and given as:

$$Ƀ_1 = (1 - \phi_{Cu} - \phi_{Go}) + \frac{\phi_{Cu}\rho_{Cu} + \phi_{Go}\rho_{Go}}{\rho_f},$$

$$Ƀ_2 = (1 - \phi_{Cu} - \phi_{Go}) + \frac{\phi_{Cu}(\rho C_p)_{Cu} + \phi_{Go}\left(\rho C_p\right)_{Go}}{(\rho C_p)_f}.$$

Dimensionless parameter are

$$N = \frac{4\sigma^* T^{*3}_{\infty}}{k_{nf} k^*_{hnf}}, \qquad Pr = \frac{\mu_f (\rho C_p)_f}{\rho_f k_f}, \qquad Mn = \frac{\bar{\sigma}_f \mathrm{B}_o^2 \mathrm{h}^2}{\rho_f \vartheta_f}, \tag{3.34}$$

$$Re = \frac{ah^2}{\upsilon}, \qquad R_o = \frac{\Omega h^2}{\vartheta_f}, \qquad Ec = \frac{\rho_f a h^2}{(\rho C_p)_f (T^*_o - T^*_H)} \tag{3.35}$$

Relevant surface constrain for model are

$$f = 0, \qquad f' = 1, \qquad g = 0, \qquad \theta = 1 \quad at \ \eta = 0, \tag{3.36}$$

$$f = A, \qquad f' = 0, \qquad g = 0, \qquad \theta = 0 \quad at \ \eta = 1. \tag{3.37}$$

Skin friction coefficient is defined as

$$C_f = \frac{\mu_{hnf}}{\rho_f v_o^2} \left.\frac{\partial u}{\partial y}\right|_{y=0}, \tag{3.38}$$

And also Nusselt number is

$$Nu = \left[\frac{h}{k_f (T^*{}_o - T^*_H)}\right] \left(k_{hnf} + \frac{16\sigma^* T^{*3}_{\infty}}{3k^*_{hnf}}\right) \left.\frac{\partial T^*}{\partial y}\right|_{y=0}. \tag{3.39}$$

We gain:

$$C^*_f = |(1 - \phi_{Cu} - \phi_{Go})^{-2.5} f''(0)\,|, \tag{3.40}$$

$$Nu^* = \left|\frac{k_{hnf}}{k_f}\left(1 + \frac{4}{3}N\right)\theta'(0)\right|. \tag{3.41}$$

3.2 Implementation of method:

We convert given order of ODE's in to first order ODE's by applying modified Adomian decomposition method and then solve analytically.

First we write higher ODE's as

$$L_4 f(\eta) = -Ƀ_1 (1 - \phi_{Cu} - \phi_{Go})^{2.5} Re(ff''' - f'f'') + 2Ƀ_1 Ro((1 - \phi_{Cu} - \phi_{Go})^{2.5} g' + Mn((1 - \phi_{Cu} - \phi_{Go})^{2.5} f'', \tag{3.42}$$

$$L_2 g(\eta) = -Ƀ_1(1-\phi_{Cu}-\phi_{Go})^{2.5}Re(fg'-f'g) - 2Ƀ_1 Ro((1-\phi_{Cu}-\phi_{Go})^{2.5}f' + Mn((1-\phi_{Cu}-\phi_{Go})^{2.5}g, \quad (3.43)$$

$$L_2\theta(\eta) = -Ƀ_2 PrRe\left(\frac{3}{3+4N}\right)\frac{k_f}{k_{hnf}}f\theta' - MnPrEc\left(\frac{3}{3+4N}\right)\frac{k_f}{k_{hnf}}(f'^2+g^2), \quad (3.44)$$

Where $L_4 = \frac{d^4}{d\eta^4}$ and $L_2 = \frac{d^2}{d\eta^2}$

Let L_4^{-1} and L_3^{-1} exist:

$$L_4^{-1}(.) = \int_0^\eta \int_0^\eta \int_0^\eta \int_0^\eta (.)d\eta d\eta d\eta d\eta \quad (3.45)$$

$$L_2^{-1}(.) = \int_0^\eta \int_0^\eta (.)d\eta d\eta \quad (3.46)$$

Putting with $L_4^{-1}$and L_2^{-1}in equation, (3.42), (3.43) and (3.44).and by applying boundary conditions we get

$$f(\eta) = f''(0)\frac{\eta^2}{2} + f'(0)\eta + L_4^{-1}(Ṅ_1 u^*) + f(0) + f'''(0)\frac{\eta^3}{6}, \quad (3.47)$$

and also

$$g(\eta) = L_2^{-1}(Ṅ_2 u^*) + g(0) + g'(0)\eta, \quad (3.48)$$

$$\theta(\eta) = L_2^{-1}(Ṅ_3 u^*) + g(0) + \theta'(0)\eta, \quad (3.49)$$

Where

$$N_1' u^* = -Ƀ_1(1-\phi_{Cu}-\phi_{Go})^{2.5}Re(ff''' - f'f'') + 2Ƀ_1 Ro((1-\phi_{Cu}-\phi_{Go})^{2.5}g' + Mn((1-\phi_{Cu}-\phi_{Go})^{2.5}f'', \quad (3.50)$$

$$N_2' u^* == -Ƀ_1(1-\phi_{Cu}-\phi_{Go})^{2.5}Re(fg'-f'g) - 2Ƀ_1 Ro((1-\phi_{Cu}-\phi_{Go})^{2.5}f' + Mn((1-\phi_{Cu}-\phi_{Go})^{2.5}g, \quad (3.51)$$

$$N_3' u^* = -\mathrm{B}_2 PrRe\left(\frac{3}{3+4N}\right)\frac{k_f}{k_{hnf}} f\theta' - MnPrEc\left(\frac{3}{3+4N}\right)\frac{k_f}{k_{hnf}}(f'^2 + g^2), \quad (3.52)$$

Now we first find the values of $f''(0)$, $f'''(0)$, $g'(0)$ and $\theta'(0)$ by using normal ADM and then put in equation (3.42), (3.43) and (3.44).

First put with L_4^{-1} on equation (3.31) at η=1 we have:

$$\int_0^1 \int_0^\eta \int_0^\eta \int_0^\eta f^{iv}(\eta) d\eta d\eta d\eta d\eta = [L_4^{-1}(N_1' u^*)]_{\eta=1}, \quad (3.53)$$

$$\int_0^1 \int_0^\eta \int_0^\eta \int_0^\eta (N_1' u^*) d\eta d\eta d\eta d\eta = [L_4^{-1}(N_1' u^*)]_{\eta=1,} \quad (3.54)$$

Integrate and by apply boundary conditions:

$$-1 - \frac{1}{2} f''(0) + A - \frac{1}{6} f'''(0) = [L_4^{-1}(N_1' u^*)]_{\eta=1} \quad (3.55)$$

First put with L_3^{-1} on equation (3.32) at η=1 we have:

$$\int_0^1 \int_0^\eta \int_0^\eta (N_1' u^*) d\eta d\eta d\eta = [L_3^{-1}(N_1' u^*)]_{\eta=1}, \quad (3.56)$$

After applying integration we get

$$-1 - f''(0) - \frac{1}{2} f'''(0) = [L_3^{-1}(N_1' u^*)]_{\eta=1} \quad (3.57)$$

By subtracting equation (3.55) from (3.57) we have.

$$f'''(0) = -6[L_3^{-1}(N_1' u^*)]_{\eta=1} - 12A + 12[L_4^{-1}(N_1' u^*)]_{\eta=1} + 6, \quad (3.58)$$

and

$$f''(0) = +2[L_3^{-1}(N_1' u^*)]_{\eta=1} + 6A - 6[L_4^{-1}(N_1' u^*)]_{\eta=1} - 4, \quad (3.59)$$

Now put $f''(0)$ and $f'''(0)$in equation (3.46) we have

$$f(\eta) = -(1-2A)\eta^3 + [L_4^{-1}(N_1{}'u^*)] + \eta + (3A-2)\eta^2 + (2\eta^3 - 3\eta^2)[L_4^{-1}(N_1{}'u^*)]_{\eta=1} + (\eta^2 - \eta^3)[L_3^{-1}(N_1{}'u^*)]_{\eta=1}, \quad (3.60)$$

So we can write it as:

$$f_o(\eta) = -(1-2A)\eta^3 + \eta + (3A-2)\eta^2,$$

$$f_{n+1}(\eta) = [L_4^{-1}(N_1{}'u^*)] + (2\eta^3 - 3\eta^2)[L_4^{-1}(N_1{}'u^*)]_{\eta=1} + (\eta^2 - \eta^3)[L_3^{-1}(N_1{}'u^*)]_{\eta=1}, \quad (3.61)$$

and also

$$g_o(\eta) = 0,$$

$$g_{n+1}(\eta) = [L_2^{-1}(N_2{}'u^*)] - \eta[L_2^{-1}(N_2{}'u^*)]_{\eta=1}, \quad (3.62)$$

For $\theta(\eta)$

$$\theta_o(\eta) = 1 - \eta,$$

$$\theta_{n+1}(\eta) = [L_2^{-1}(N_3{}'u^*)] - \eta[L_2^{-1}(N_3{}'u^*)]_{\eta=1}. \quad (3.65)$$

Using Maple software for analytical solution of the problem.

Table2. Contrast between present and Ref.6 results of Nusselt number.

	Re	*N*, *Mn*=0, *Ec*=0	6 results
$\emptyset = 0\%$	0.1	1.078381555	1.07650
	0.5	1.403658578	1.40437
	1	1.813100376	1.81603
	1.5	2.201327214	2.20219
$\emptyset = 5\%$	0.1	1.298621376	1.29872
	0.5	1.619052807	1.29872
	1	2.026519802	2.02732
	1.5	2.422539174	2.42441
$\emptyset = 10\%$	0.1	1.573849277	1.57195
	0.5	1.889474207	1.88889
	1	1.889474207	2.29326
	1.5	2.292857255	2.29326
		2.691972738	2.69399

3.3 Results and discussion

Fluid flow is considered between two parallel plates in which the upper wall is stretchable and other is penetrable and also under the influence of thermal radiation and joule heating. Heat transfer and MHD hybrid nanofluid flow are study analytically. Different parameters which includes rotation (R_o), radiation (N), magnetic (Mn), Reynolds number (Re), suction\injection (A) and hybrid nanofluid volume fraction ($\emptyset$) are explored concerning the flow and heat transfer. Detail of thermo physical properties are discussed in Table.1.It is noted that equal volume fraction of graphene oxide and cupper ($\emptyset_{Cu} = \emptyset_{Go} = 0.5\emptyset$) are utilized. Solution is obtained by using analytical technique and then MAPLE is used for graphical representation to see the effects of velocity and temperature profile for different parameter.

Figure. (3.2) and (3.3) shows the effect of A and Re on velocity profile f and g accordingly. It is mention earlier that $A>0$ shows the injection flow and $A<0$ shows the suction flow from upper wall. One can see that, if values of injection parameter increases then velocity profile also rises. While for suction parameter, increase in value of suction parameter causes decrease in velocity profile. Contrastingly, for injection process g decreases and f increases when Re number increases. Moreover, for small value of Re, the g shows centerline symmetry while at larger value of Re, higher velocity point moves to upper wall.

Figure. (3.4) and (3.5). Indicate the impact of Re and A on temperature profile and Nusselt number. For injection process temperature profile decreases and Nusselt number increases while for suction process Nusselt number goes down. With ascending Re, θ will diminish .The results also indicate that shear stress increases and Nusselt number goes up with an increase in Reynolds number. Although, this is valid for any value of injection parameter and for small value of suction parameter. Also Nusselt number become decreasing function of Re for larger value of suction parameter.

In Figure. (3.6) and (3.7) the impact of Mn and R_o on velocity profile are discussed. Experienced that, by increasing Mn, the Lorentz force also rises and resist more effectively to the flow. In this manner the velocity profile will be degraded by increasing Mn. This is introduce in Figure. (3.7). It tends to be additionally conclude that climbing upside of rotation parameter causes increase in g and decrease in$f$. In any case, this is valid for variety of f for rotation parameter at $\eta > 0.3$. But For $\eta < 0.3$ the value of f become increases. Figure. (3.8) and (3.9) depict that, the rising qualities of magnetic and rotation parameter cause the thermal boundary layer to be condense, bringing about the temperature profile's increases with an expanding in the magnetic and rotation parameter.

In addition, in light of the fact that the Nusselt number and the thermal boundary layer thickness have a rearranged relationship, the Nusselt number lessens with increasing Mn also, R_o.

Figure. (3.10) and (3.11). Depicts $R_o$and ϕ impact on Nusselt number and temperature profile. An increase in value of R_o and ϕ of hybrid nanofluid cause an increase in hybrid nanofluid temperature. Accordance to Eq. (3.41), the Nusselt number is pronounced as an intensification of $(\frac{k_{nf}}{k_f})$, $((4/3)N+1)$ and $\theta'(0)$. As increasing the value of hybrid nanofluid volume fraction cause an increase in $(\frac{k_{nf}}{k_f})$ which is higher than the decreasing value of $\theta'(0)$ for certain value of N and also by raising the value of N results decrease in $\theta'(0)$ which is smaller than increasing value of $((4/3)N+1)$ for certain value of ϕ. So we can securely count that the Nusselt number increases with increasing hybrid nanofluids N and ϕ. Hence we find Nusselt number as an active parameter in our study.

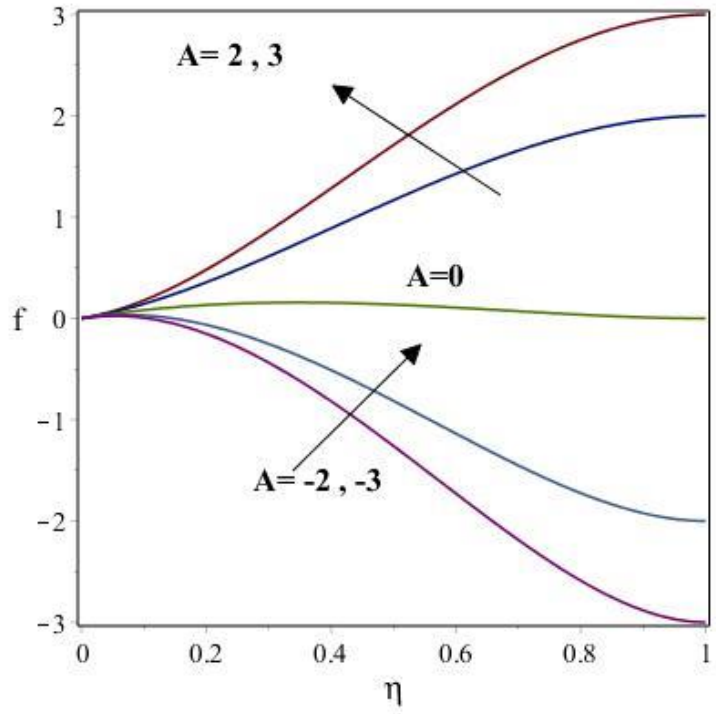

(a)

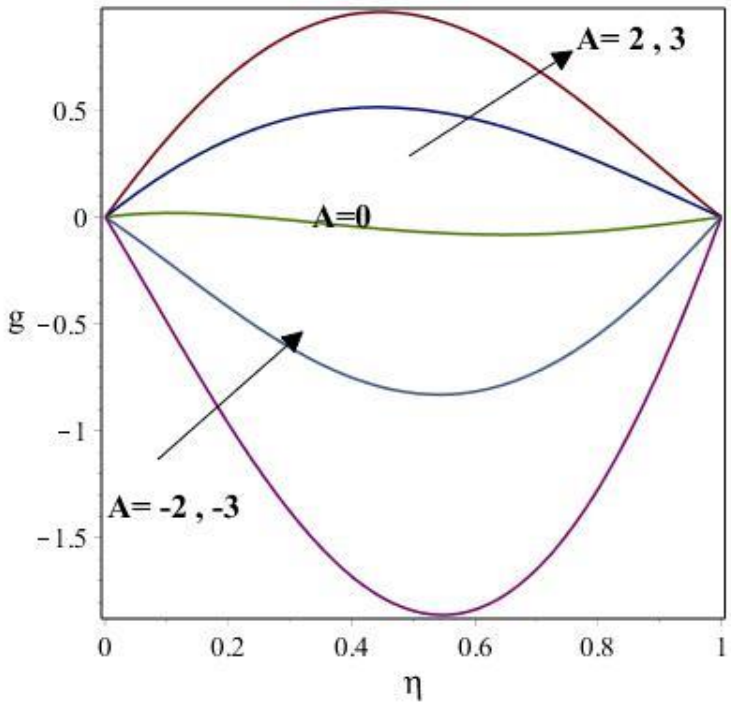

(b)

Figure.(3.2). Variation of suction/injection parameter with velocity profile (a) $f(\eta)$and (b) $g(\eta)$.

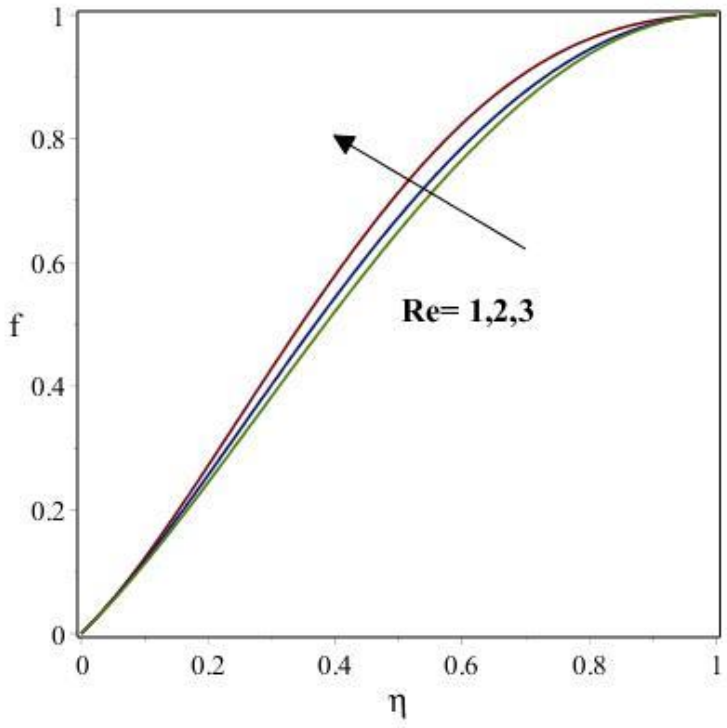

(a)

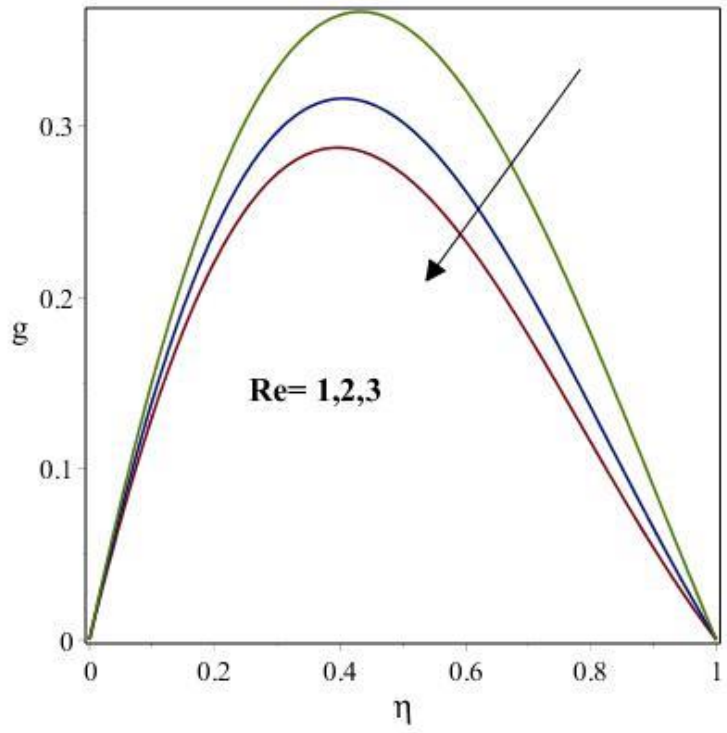

(b)

Figure.(3.3). Variation of Reynold number with velocity profiles (a) $f(\eta)$and (b) $g(\eta)$..

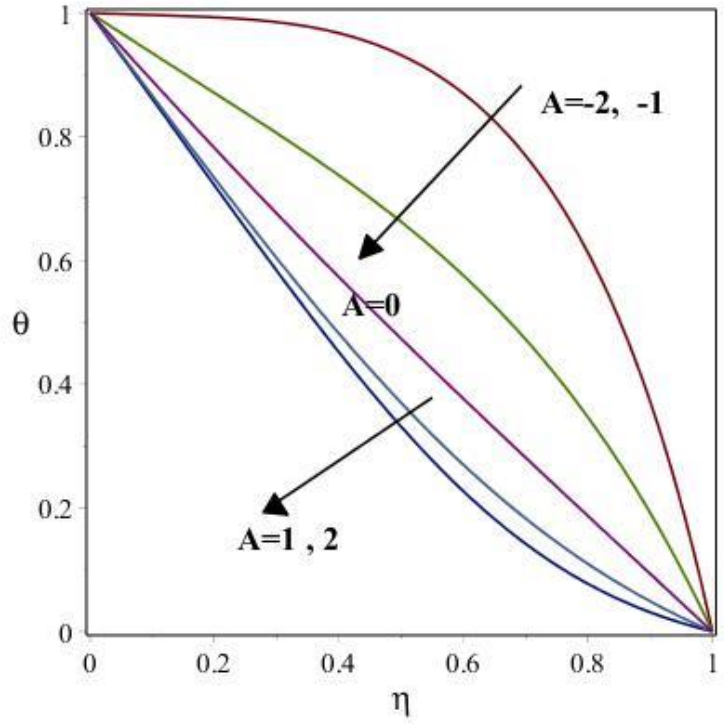

(a)

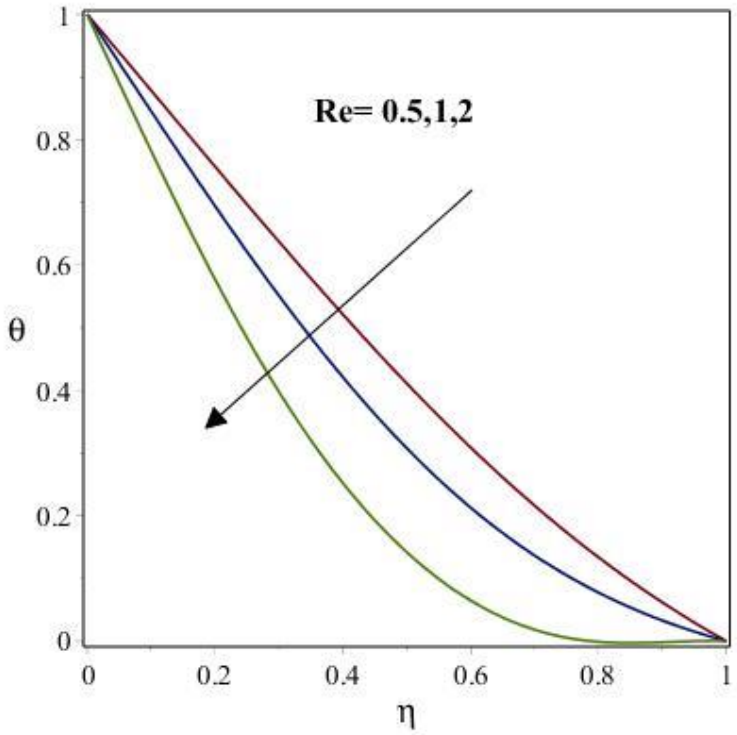

(b)

Figure. (3.4). Influence of (a) *A* and (b) *Re* on the temperature profile.

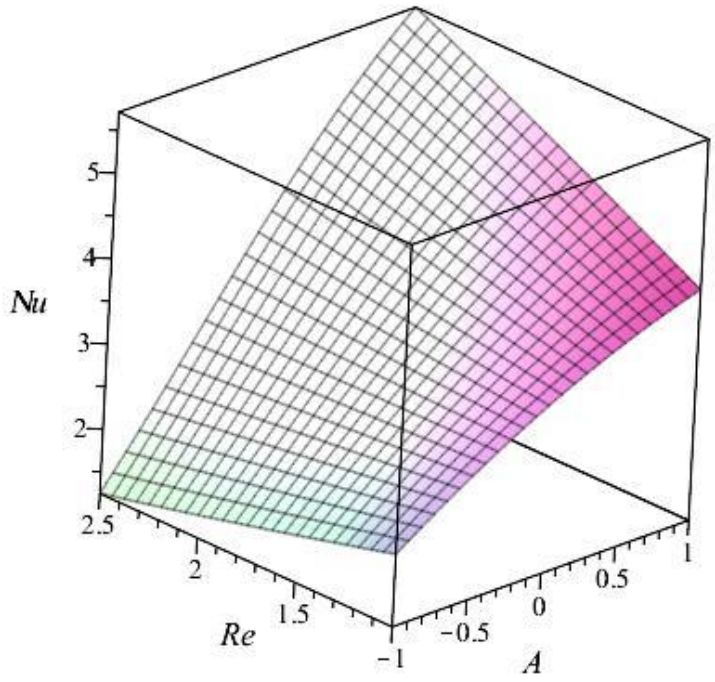

(a)

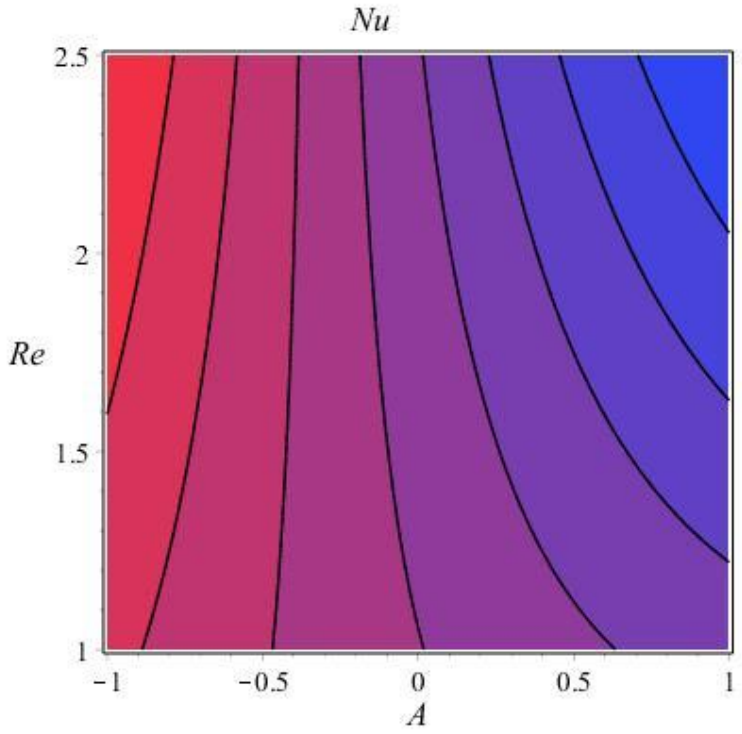

(b)

Figure. (3.5). Variation of (a) *A* and (b) Reynolds number with Nusselt number.

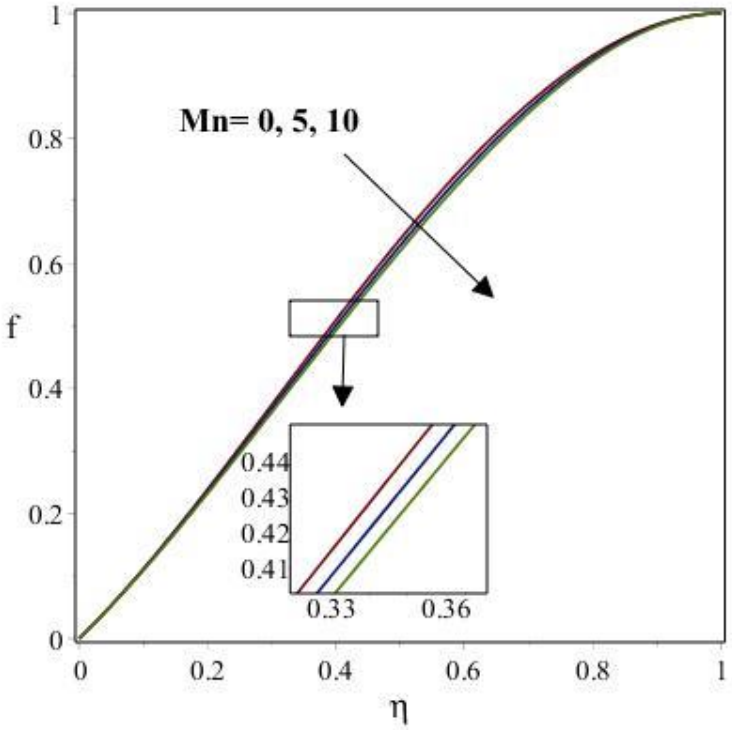

(a)

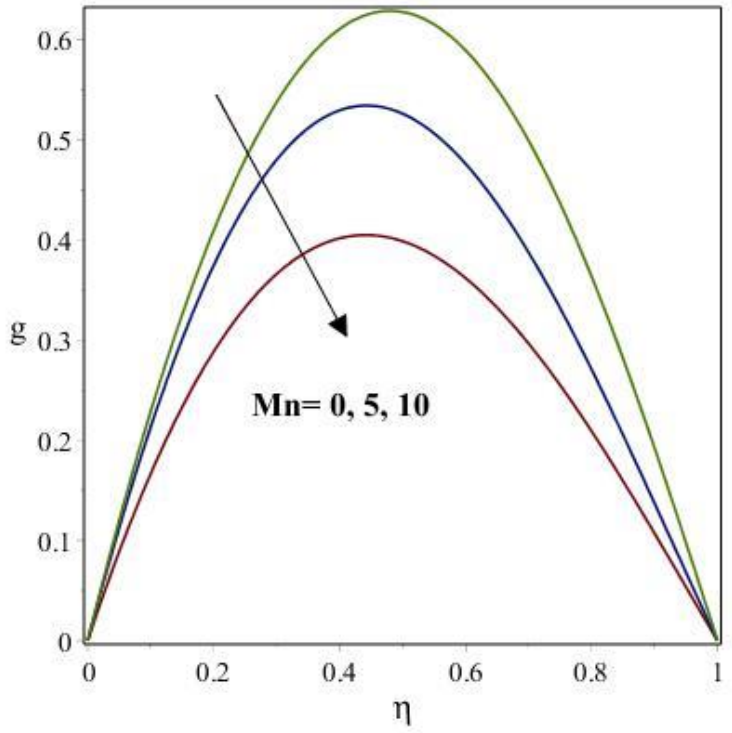

(b)

Figure.(3.6). variation of magnatic parameter with (a) $f(\eta)$and (b) $g(\eta)$.

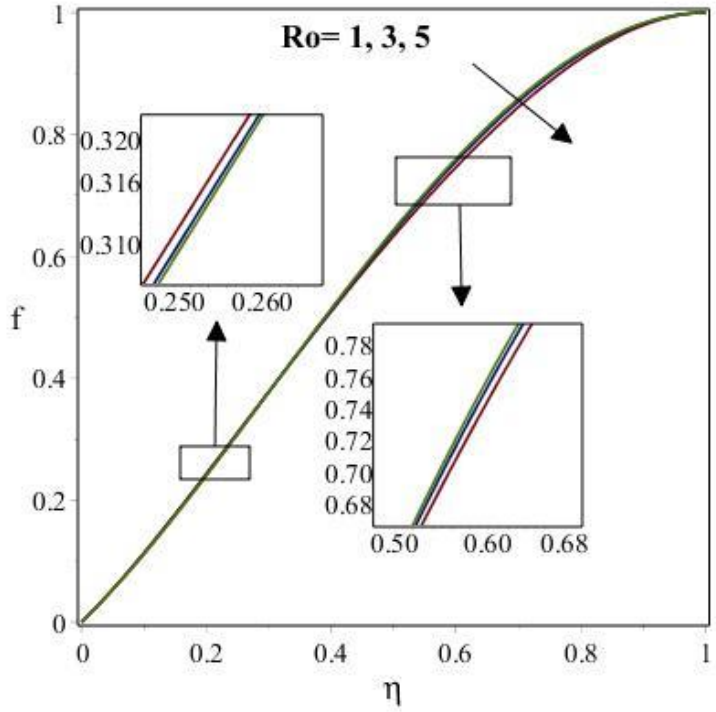

(a)

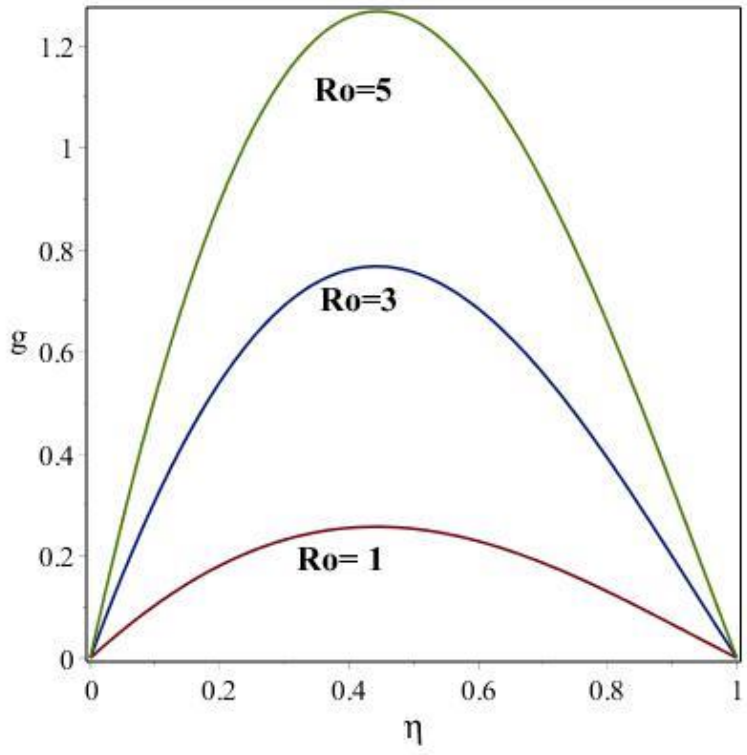

(b)

Figure.(3.7). Variation of Rotation parameter with velocity profile (a) $f(\eta)$and (b) $g(\eta)$.

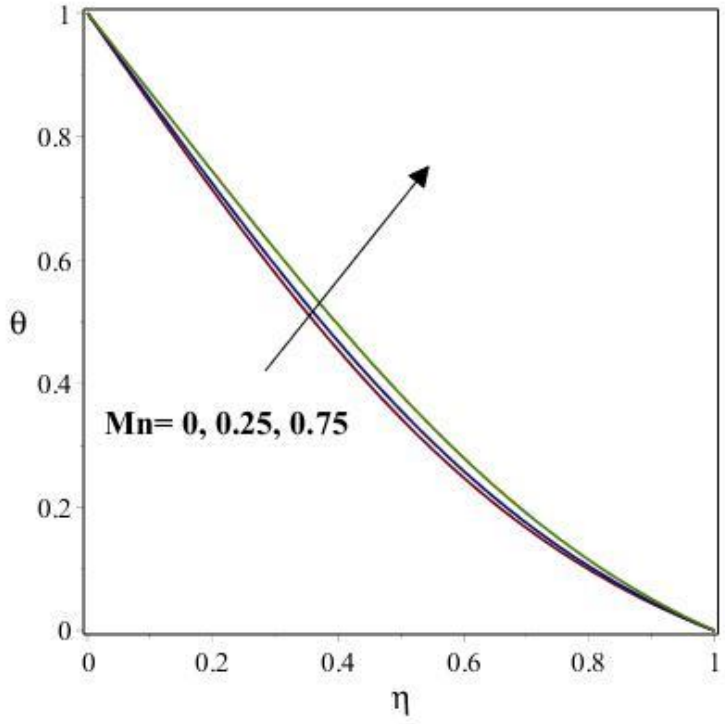

(a)

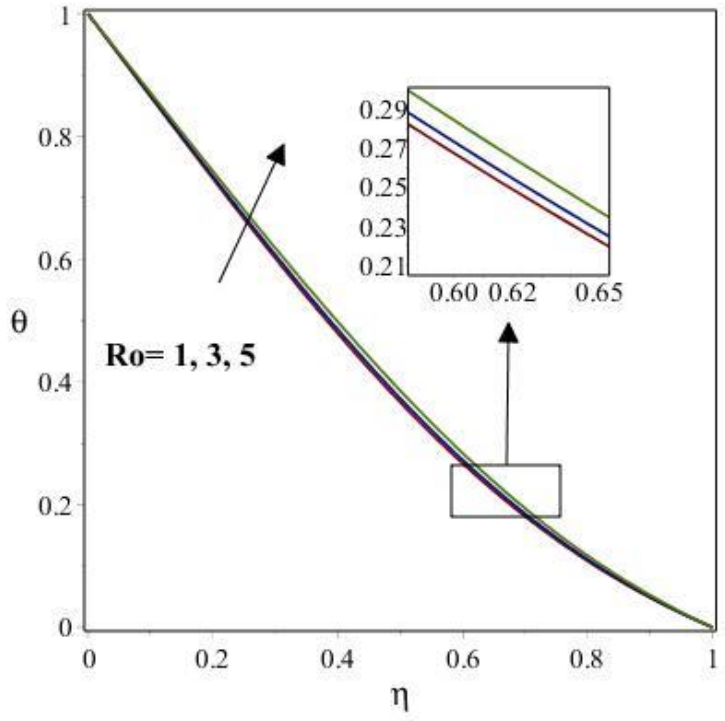

(b)

Figure. (3.8). Influence of (a) magnetic and (b) rotation parameters on the temperature profile.

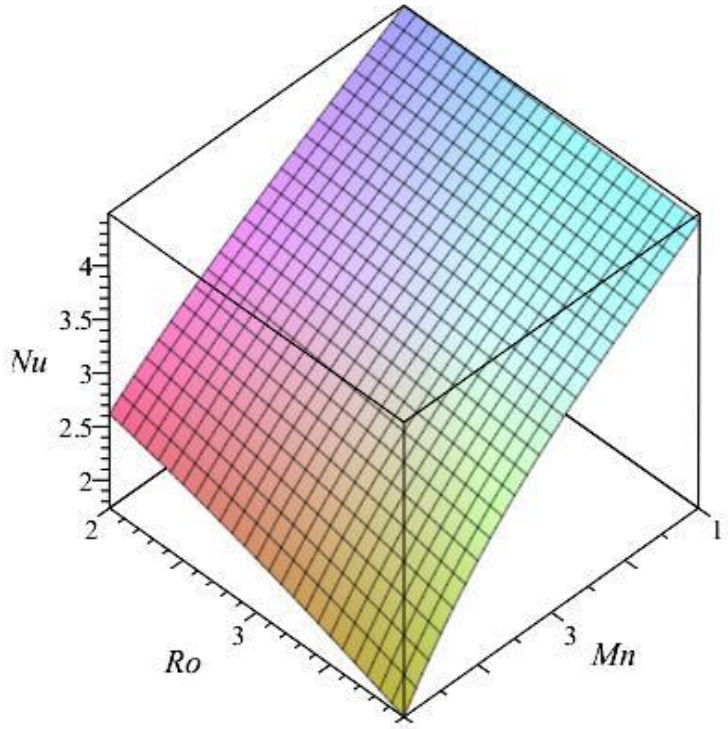

(a)

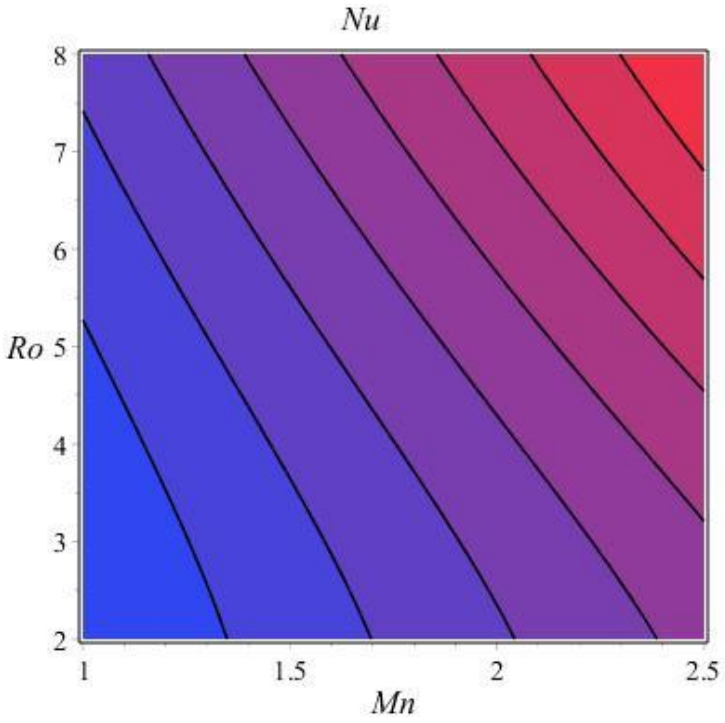

(b)

Figure. (3.9). Influence of (a) magnetic and (b) rotation parameters on the Nusselt number.

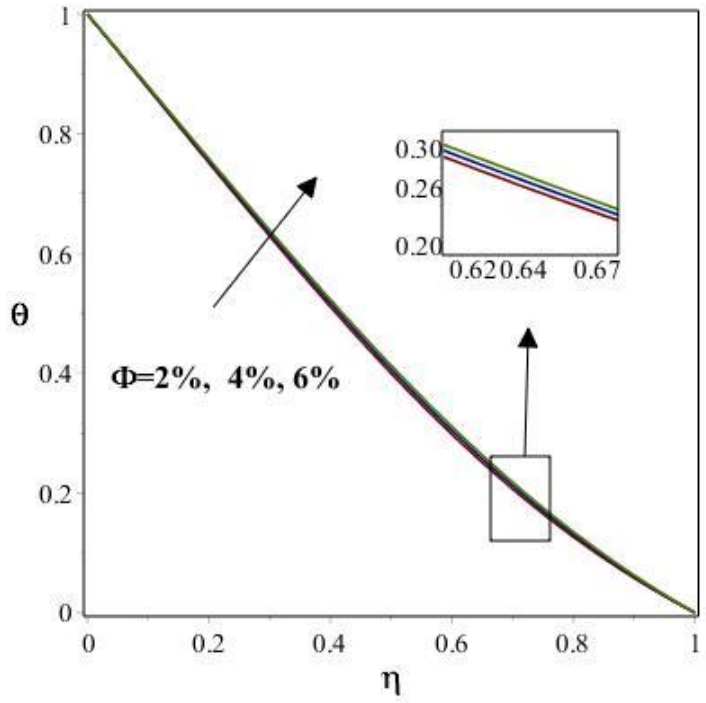

(a)

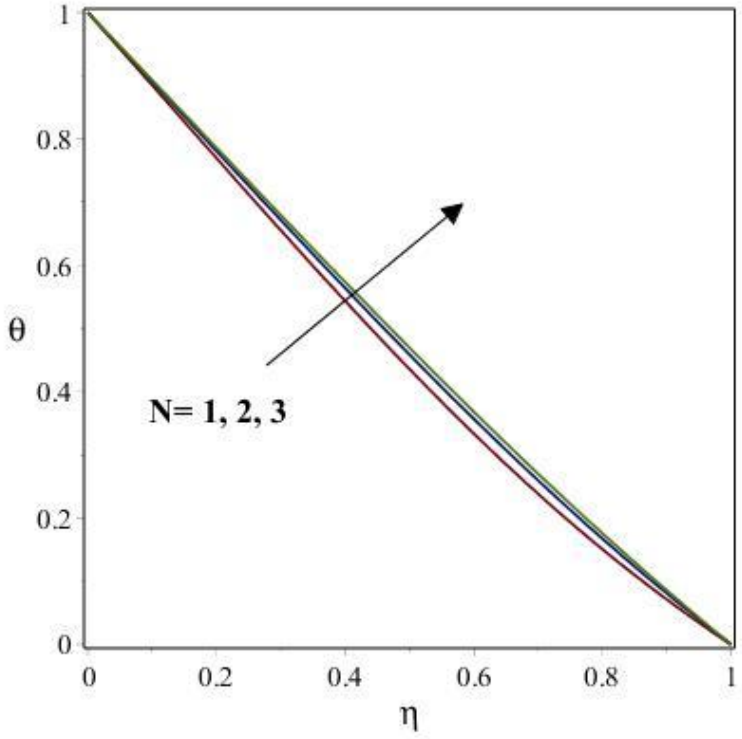

(b)

Figure. (3.10). Influence of (a) N and (b) ϕ on the temperature profile.

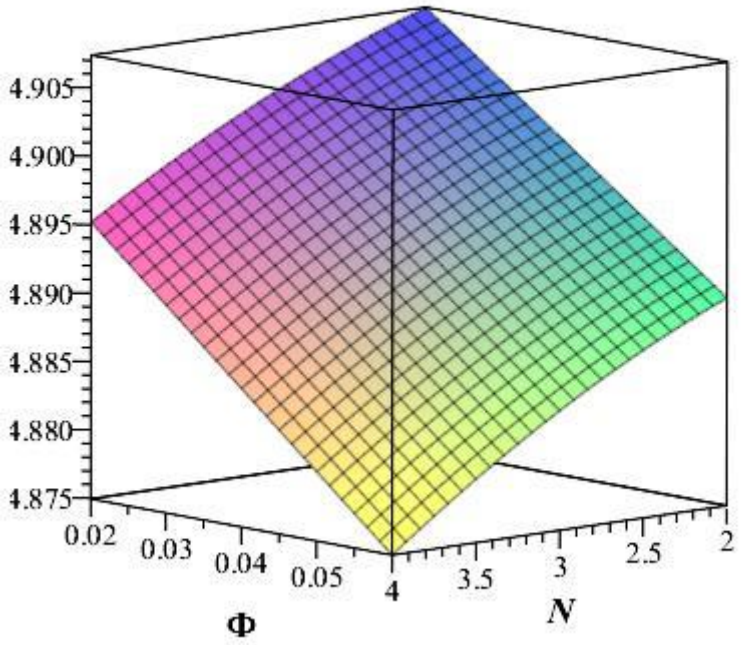

(a)

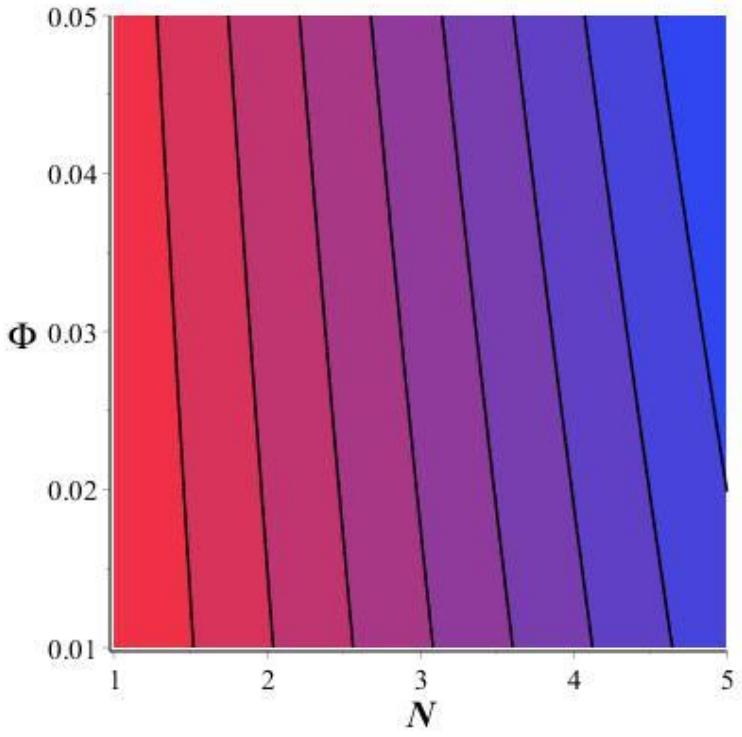

(b)

Figure. (3.11). influence of solid volume fraction on Nusselt number.

Chapter 4

Thermal performance of hybrid nanofluid in a rotating vertical channel between two plates

This chapter is extension of previous chapter by adding new terms of mixed convection and heat generation\absorption. Based upon previous chapter 3 the mathematical model rearranged and new effect has included. Results are obtained by analytical technique.

4.1 Modeling of problem

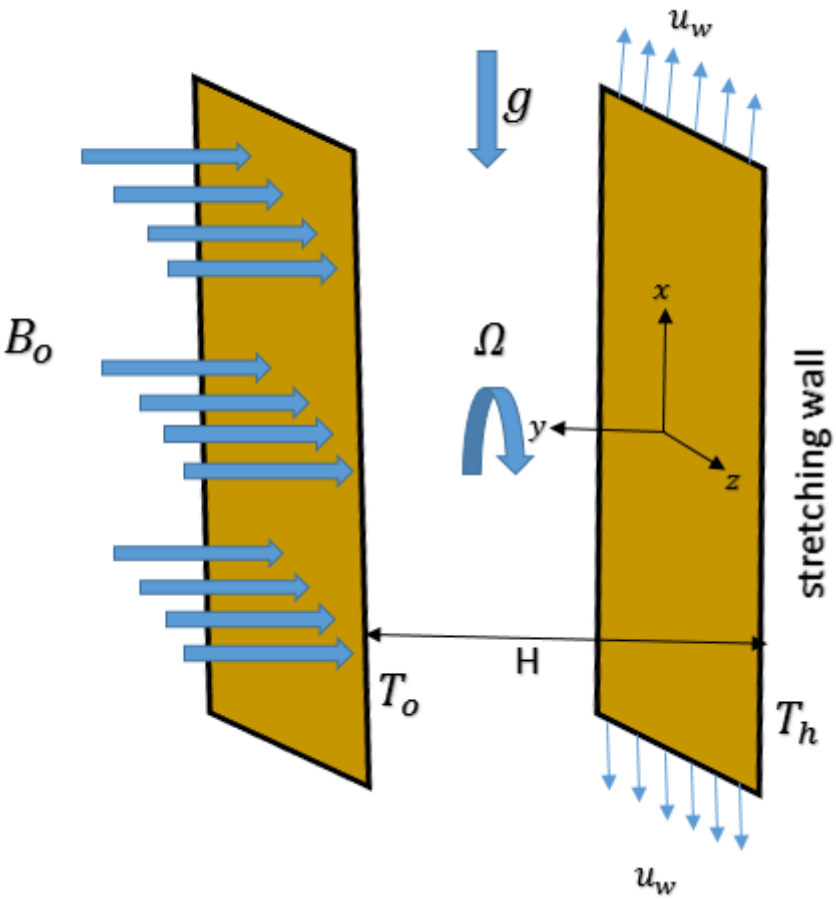

4.1: Geometry of problem

Consider steady, incompressible flow between two vertical plates. Due to rotation of channel fluid is rotating with velocity Ω. Motion of the plate is due to velocity $u^* = ax$.

The governing equation of energy and momentum are:

$$\frac{\partial v^*}{\partial y} + \frac{\partial u^*}{\partial x} = 0 \tag{4.1}$$

$$v^* \frac{\partial u^*}{\partial y} + u^* \frac{\partial u^*}{\partial x} + 2\Omega \mathrm{w}^* = -\frac{1}{\rho_{hnf}} \frac{\partial P}{\partial x} + \frac{\mu_{hnf}}{\rho_{hnf}} \left(\frac{\partial^2 u^*}{\partial x^2} + \frac{\partial^2 u^*}{\partial y^2} \right) - \frac{\bar{\sigma}_f B_o^2}{\rho_{hnf}} u^* + \frac{g(\rho\beta)_{hnf}(T^* - T_o^*)}{\left(\rho C_p\right)_{hnf}}, \tag{4.2}$$

$$v^* \frac{\partial v^*}{\partial y} + u^* \frac{\partial v^*}{\partial x} = -\frac{1}{\rho_{hnf}} \frac{\partial P}{\partial y} + \frac{\mu_{hnf}}{\rho_{hnf}} \left(\frac{\partial^2 v^*}{\partial x^2} + \frac{\partial^2 v^*}{\partial y^2} \right), \tag{4.3}$$

$$v^* \frac{\partial w^*}{\partial y} + u^* \frac{\partial w^*}{\partial x} - 2\Omega \mathrm{u}^* = \frac{\mu_{hnf}}{\rho_{hnf}} \left(\frac{\partial^2 u^*}{\partial x^2} + \frac{\partial^2 u^*}{\partial y^2} \right) - \frac{\bar{\sigma}_f B_o^2}{\rho_{hnf}} w^*, \tag{4.4}$$

$$v^* \frac{\partial T^*}{\partial y} + u^* \frac{\partial T^*}{\partial x} = \frac{k_{hnf}}{\left(\rho C_p\right)_{hnf}} \left(\frac{\partial^2 T^*}{\partial x^2} + \frac{\partial^2 T^*}{\partial y^2} \right) - \frac{1}{\left(\rho C_p\right)_{hnf}} \frac{\partial q_{rad}^*}{\partial y} + \frac{\bar{\sigma}_f B_o^2}{\left(\rho C_p\right)_{hnf}} \left(u^{*2} + w^{*2} \right) + \frac{Q(T^* - T_o)}{\left(\rho C_p\right)_{hnf}}, \tag{4.5}$$

In equations Ω is angular velocity, u^*, v^* and w^* are velocities in x, y and z directions, B_o is magnetic field, P is pressure, T^* is temperature, $\bar{\sigma}_f$ is electrical conductivity and q_{rad}^* demonstrate radiative heat flux.

For radiation

$$q_{rad}^* = -\left(\frac{4\sigma^*}{3k_{hnf}^*} \right) \frac{\partial T^{*4}}{\partial y}, \tag{4.6}$$

We can expand T^{*4} in a Taylor series and by this expansion we get

$$T^{*4} \cong -3T_\infty^{*4} + 4T_\infty^{*3} T^*. \tag{4.7}$$

So the equation (4.5) become

$$v^*\frac{\partial T^*}{\partial y}+u^*\frac{\partial T^*}{\partial x}+w^*\frac{\partial T^*}{\partial z}$$
$$=\frac{k_{hnf}}{(\rho C_p)_{hnf}}\left(\frac{\partial^2 T^*}{\partial x^2}+\frac{\partial^2 T^*}{\partial y^2}+\frac{\partial^2 T^*}{\partial z^2}\right)+\frac{16\sigma^* T_\infty^{*3}}{3k_{nf}^*(\rho C_p)_{nf}}\frac{\partial^2 T^*}{\partial y^2}+\frac{\bar{\sigma}_f B_o^2}{(\rho C_p)_{hnf}}(u^{*2}+w^{*2})$$
$$+\frac{Q(T^*-T_o^*)}{(\rho C_p)_{hnf}}. \quad (4.8)$$

Effective dynamic viscosity, heat capacity and thermal conductivity are define as:

$$\rho_{hnf}=(1-\phi_{Cu}-\phi_{Go})\rho_f+\phi_{Cu}\rho_{Cu}+\phi_{Go}\rho_{Go}, \quad (4.9)$$

$$(\rho C_p)_{hnf}=(1-\phi_{Cu}-\phi_{Go})(\rho C_p)_f+\phi_{Cu}(\rho C_p)_{Cu}+\phi_{Go}(\rho C_p)_{Go}, \quad (4.10)$$

$$\mu_{nf}=\mu_f(1-\phi_{Cu}-\phi_{Go})^{-2.5}, \quad (4.11)$$

$$\frac{k_{hnf}}{k_f}=\left\{\frac{k_{Cu}\phi_{Cu}+k_{Go}\phi_{Go}}{\phi_{Cu}+\phi_{Go}}+2k_f+2(k_{Cu}\phi_{Cu}+k_{Go}\phi_{Go})\right.$$
$$\left.-2(\phi_{Cu}+\phi_{Go})k_f\right\}\left\{\frac{k_{Cu}\phi_{Cu}+k_{Go}\phi_{Go}}{\phi_{Cu}+\phi_{Go}}+2k_f-(k_{Cu}\phi_{Cu}+k_{Go}\phi_{Go})\right.$$
$$\left.+(\phi_{Cu}+\phi_{Go})k_f\right\}^{-1}, \quad (4.12)$$

$$(\rho\beta)_{hnf}=(1-\phi_{Cu}-\phi_{Go})(\rho\beta)_f+\phi_{Cu}(\rho\beta)_{Cu}+\phi_{Go}(\rho\beta)_{Go}. \quad (4.13)$$

Table1. Thermo physical properties of hybrid nanofluid and water.

	(kg/m^3)	**C_p(J/kg K)**	**k(W/m k)**
Graphene Oxide (Go)	1800	717	5000
Copper (Cu)	8933	385	401
Pure water	997.1	4179	0.613

Boundary conditions at lower and upper surfaces are:

$$u^*=u_w^*=ax, \quad v^*=0, \quad w^*=0, \quad T^*=T_H^* \quad at\ y=0 \quad (4.14)$$

$$u^*=0, \quad v^*=v_o, \quad w^*=0, \quad T^*=T_o^* \quad at\ y=h \quad (4.15)$$

Using similarity variables:

$$\eta = \frac{y}{h}, \quad v^* = -ahf(\eta), \qquad u^* = axf'(\eta)\; w^* = axg(\eta) \quad \theta = \frac{T^* - T_H^*}{T_o^* - T_H^*}. \tag{4.16}$$

By using similarity variables the given PDE's transformed in to dimensionless ODE's.

$$f^{iv} + \text{Ƀ}_1(1-\phi_{Cu}-\phi_{Go})^{2.5}Re(ff''' - f'f'') - 2\text{Ƀ}_1 R_o((1-\phi_{Cu}-\phi_{Go})^{2.5}g' - Mn((1-\phi_{Cu}-\phi_{Go})^{2.5}f'' + GrRe\text{Ƀ}_1'(1-\phi_{Cu}-\phi_{Go})^{2.5}\theta' = 0, \tag{4.17}$$

$$g'' + \text{Ƀ}_1(1-\phi_{Cu}-\phi_{Go})^{2.5}Re(fg' - f'g) + 2\text{Ƀ}_1 R_o((1-\phi_{Cu}-\phi_{Go})^{2.5}f' - Mn((1-\phi_{Cu}-\phi_{Go})^{2.5}g = 0, \tag{4.18}$$

$$\theta'' + \text{Ƀ}_2 PrRe\left(\frac{3}{3+4N}\right)\frac{k_f}{k_{hnf}}f\theta' + MnPrEc\left(\frac{3}{3+4N}\right)\frac{k_f}{k_{hnf}}(f'^2 + g^2) + Q_o PrRe\left(\frac{3}{3+4N}\right)\frac{k_f}{k_{hnf}}\theta = 0. \tag{4.19}$$

Ƀ_1 , Ƀ_1^* and Ƀ_2 are constant and given as:

$$\text{Ƀ}_1 = (1-\phi_{Cu}-\phi_{Go}) + \frac{\phi_{Cu}\rho_{Cu} + \phi_{Go}\rho_{Go}}{\rho_f}$$

$$\text{Ƀ}_1^* = (1-\phi_{Cu}-\phi_{Go})(\rho\beta)_f + \frac{\phi_{Cu}(\rho\beta)_{Cu} + \phi_{Go}(\rho\beta)_{Go}}{(\rho\beta)_f}$$

$$\text{Ƀ}_2 = (1-\phi_{Cu}-\phi_{Go}) + \frac{\phi_{Cu}(\rho C_p)_{Cu} + \phi_{Go}(\rho C_p)_{Go}}{(\rho C_p)_f}$$

Dimensionless parameter are:

$$N = \frac{4\sigma^* T_\infty^3}{k_{nf}k_{hnf}^*}, \; Pr = \frac{\mu_f(\rho C_p)_f}{\rho_f k_f}, \; Mn = \frac{\bar{\sigma}_f \mathrm{B_o^2 h^2}}{\rho_f \vartheta_f}, \tag{4.20}$$

$$Re = \frac{ah^2}{\upsilon}, \qquad R_o = \frac{\Omega h^2}{\vartheta_f}, \qquad Ec = \frac{\rho_f a h^2}{(\rho C_p)_f(T_o^* - T_H^*)}. \tag{4.21}$$

Relevant surface constrain for model are

$$f = 0,\; f' = 1, \qquad g = 0, \qquad \theta = 1 \quad at\;\eta = 0, \tag{4.22}$$

$$f = A, \quad f' = 0, \quad g = 0, \quad \theta = 0 \quad at\;\eta = 1. \tag{4.23}$$

Skin friction coefficient is defined as

$$C_f = \frac{\mu_{hnf}}{\rho_f v_o^2} \frac{\partial u}{\partial y}\bigg|_{y=0}, \tag{4.24}$$

And also Nusselt number is

$$Nu = \left[\frac{h}{k_f(T_o - T_H)}\right]\left(k_{hnf} + \frac{16\sigma^* T^{*3}_{\infty}}{3k^*_{hnf}}\right)\frac{\partial T^*}{\partial y}\bigg|_{y=0}. \tag{4.25}$$

We gain:

$$C_f^* = |(1 - \phi_{Cu} - \phi_{Go})^{-2.5} f''(0)\,|, \tag{4.26}$$

$$Nu^* = \left|\frac{k_{hnf}}{k_f}\left(1 + \frac{4}{3}N\right)\theta'(0)\right|. \tag{4.27}$$

(4.2) Methodology

In this section, same method (ADM) is adopted as we have discussed in chapter 3. In order to avoid the repetition of method, we just mentioned the initial guess of modified model for velocities and temperature and then define the operators that is used to solve the given system of equations (4.17)-(4.19) with boundary conditions (4.22) and (4.23).

Simplifying the fourth order ODE's by using the similar technique (ADM) we get.

Let

$$f^{iv} = -Ƀ_1(1 - \phi_{Cu} - \phi_{Go})^{2.5} Re(ff''' - f'f'') - 2Ƀ_1 R_o((1 - \phi_{Cu} - \phi_{Go})^{2.5} g' - Mn((1 - \phi_{Cu} - \phi_{Go})^{2.5} f'' + GrReɃ_1'(1 - \phi_{Cu} - \phi_{Go})^{2.5}\theta' = 0, \tag{4.28}$$

$$g'' = -Ƀ_1(1 - \phi_{Cu} - \phi_{Go})^{2.5} Re(fg' - f'g) - 2Ƀ_1 Ro((1 - \phi_{Cu} - \phi_{Go})^{2.5} f' + Mn((1 - \phi_{Cu} - \phi_{Go})^{2.5} g, \tag{4.29}$$

$$\theta'' = -Ƀ_2 PrRe\left(\frac{3}{3 + 4N}\right)\frac{k_f}{k_{hnf}} f\theta' - MnPrEc\left(\frac{3}{3 + 4N}\right)\frac{k_f}{k_{hnf}}(f'^2 + g^2) - Q_o PrRe\left(\frac{3}{3 + 4N}\right)\frac{k_f}{k_{hnf}}\theta = 0. \tag{4.30}$$

Operators for f, g and θ,

$f^{iv} = L_4 f = \frac{d^4}{d\eta^4} f$, $g'' = L_2 f = \frac{d^2}{d\eta^2} g$, and $\theta'' = L_2 f = \frac{d^2}{d\eta^2}\theta$.

And inverse operators are $L_4^{-1}(.) = \int_0^\eta \int_0^\eta \int_0^\eta \int_0^\eta (.) d\eta d\eta d\eta d\eta$ and $L_3^{-1}(.) = \int_0^\eta \int_0^\eta \int_0^\eta (.) d\eta d\eta d\eta$

Now the initial guess are

$$f_o(\eta) = -(1-2A)\eta^3 + \eta + (3A-2)\eta^2,$$

$$f_{n+1}(\eta) = [L_4^{-1}(N_1{}'u^*)] + (2\eta^3 - 3\eta^2)[L_4^{-1}(N_1'u^*)]_{\eta=1} + (\eta^2 - \eta^3)[L_3^{-1}(N_1{}'u^*)]_{\eta=1}, \quad (4.31)$$

$$g_o(\eta) = 0,$$

$$g_{n+1}(\eta) = [L_2^{-1}(N_2{}'u^*)] - \eta[L_2^{-1}(N_2'u^*)]_{\eta=1}, \quad (4.32)$$

$$\theta_o(\eta) = 1 - \eta,$$

$$\theta_{n+1}(\eta)[L_2^{-1}(N_3{}'u^*)] - \eta[L_2^{-1}(N_3{}'u^*)]_{\eta=1}. \quad (4.33)$$

where

$$N_1{}'u^* = -\text{Ƀ}_1(1-\phi_{Cu}-\phi_{Go})^{2.5}Re(ff''' - f'f'') + 2\text{Ƀ}_1Ro((1-\phi_{Cu}-\phi_{Go})^{2.5}g' + Mn((1-\phi_{Cu}-\phi_{Go})^{2.5}f'' + GrRe\text{Ƀ}_1'(1-\phi_{Cu}-\phi_{Go})^{2.5}\theta', \quad (4.34)$$

$$N_2'u^* = -\text{Ƀ}_1(1-\phi_{Cu}-\phi_{Go})^{2.5}Re(fg' - f'g) - 2\text{Ƀ}_1Ro((1-\phi_{Cu}-\phi_{Go})^{2.5}f' + Mn((1-\phi_{Cu}-\phi_{Go})^{2.5}g, \quad (4.35)$$

$$N_3'u^* = -\text{Ƀ}_2PrRe\left(\frac{3}{3+4N}\right)\frac{k_f}{k_{hnf}}f\theta' - MnPrEc\left(\frac{3}{3+4N}\right)\frac{k_f}{k_{hnf}}(f'^2 + g^2) + Q_oPrRe\left(\frac{3}{3+4N}\right)\frac{k_f}{k_{hnf}}\theta\,. \quad (4.36)$$

Using Maple to solve the problem

4.3 Results and discussion

Former, the nonlinear PDE's are reconstructed in to ODE's and analytical technique is use for the solution of problem. Impact of magnetic parameter, suction/injection parameter, Reynolds number, and Rotation parameter on velocity profile, temperature profile and Nusselt number examined. The effect of *A* and Re on velocity profile f and g are shown in Figure. (4.2) and (4.3). It is mention earlier that *A*>0 shows the injection flow and *A*<0 shows the suction flow. If values of injection parameter goes up then velocity profile also rises in *x* and *y*-direction. While for suction parameter, increase in value of suction parameter causes decrease in velocity profile. For injection

process g decreases and f increases when Re number increases. Moreover, for small value of Re, the g decreases while at larger value of Re, higher velocity point moves.

Figure. (4.4) and (4.5) indicate the impact of Re and injection parameter on temperature profile and Nusselt number. For injection process temperature profile decreases and Nusselt number increases while for suction process Nusselt number goes down. With ascending Re, θ will diminish .The results also indicate that shear stress increases and Nusselt number goes up with an increase in Reynolds number. Although, this is valid for any value of injection parameter and for small value of suction parameter. Also Nusselt number become decreasing function of Re for larger value of suction parameter.

In Figure. (4.6) and (4.7) the impact of Mn and R_o on velocity profile are discussed. Experienced that, by increasing Mn, the Lorentz force also rises and resist more effectively to the flow. In this manner, one can see that velocity profile will be degraded by increasing Mn. This is introduce in Figure. (4.6). It tends to be additionally conclude that climbing upside of rotation parameter causes increase in g and decrease in f. In any case, this is valid for variety of f for rotation parameter at $\eta > 0.3$. But For $\eta < 0.3$ the value of f become increases. Figure. (4.8) and (4.9) depict that, the rising qualities of magnetic and rotation parameter cause the thermal boundary layer to be condense, bringing about the temperature profile's increases with an expanding in the magnetic and rotation parameter. In addition, in light of the fact that the Nusselt number and the thermal boundary layer thickness have a rearranged relationship, the Nusselt number increases with increasing Mn and R_o. Figure. (4.10) and (4.11). Demonstrate the effect of N and solid volume fraction on temperature profile and Nusselt number. An increment in value of N and solid volume fraction cause increase in temperature profile. Nusselt number will also increases with increasing the value of N and solid volume fraction.

The influence of Grashaf number on velocity profile and temperature are shown in Figure.(4.12) and (4.13). It is clear from graphical representation that when Grashaf number rises the velocity in x-direction also rises. While velocity profile in z-direction decreases with increasing the value of Grashaf number. The relation of Grashaf number with temperature profile are shown in figure, (4.13). It demonstrate that temperature profile will also increase with increasing Grashaf number.

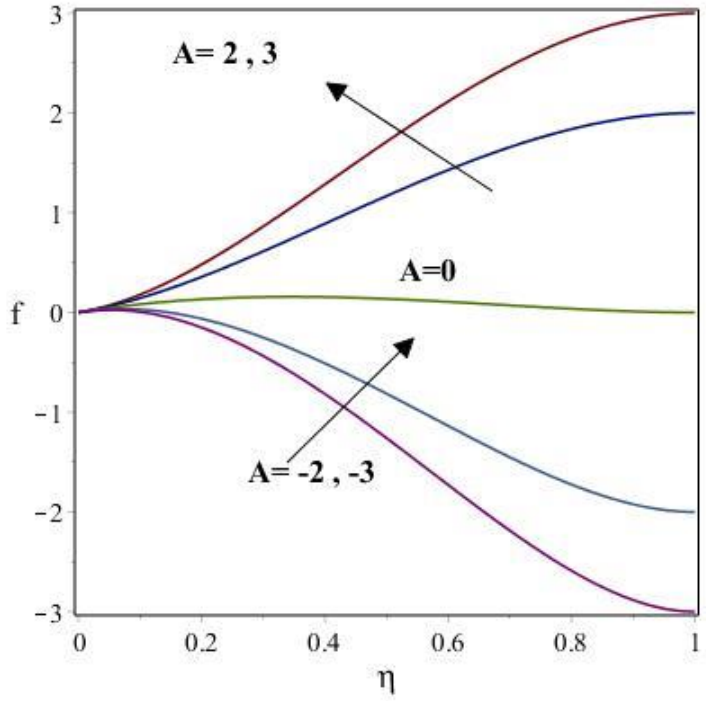

(a)

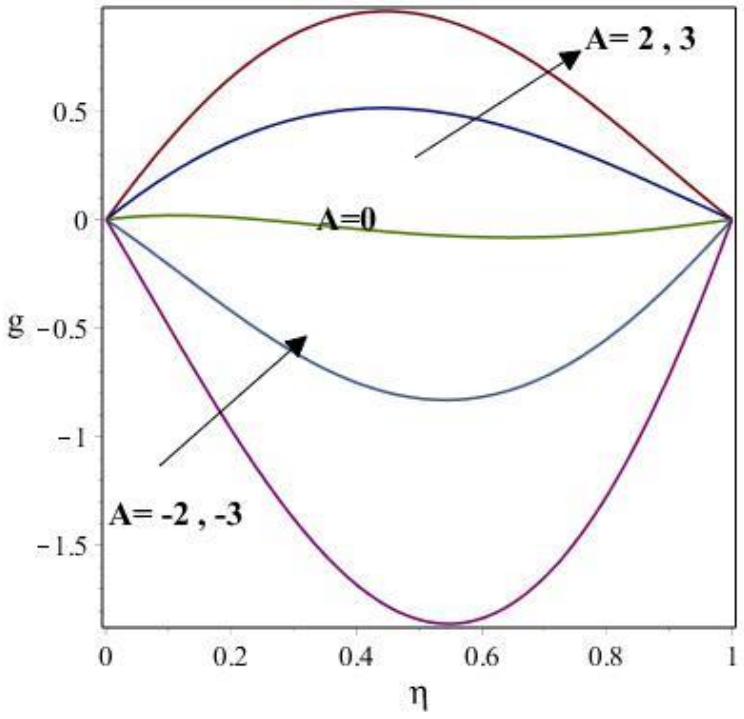

(b)

Figure.(4.2). variation of suction/injection parameter with velocity profile (a) $f(\eta)$ and (b) $g(\eta)$.

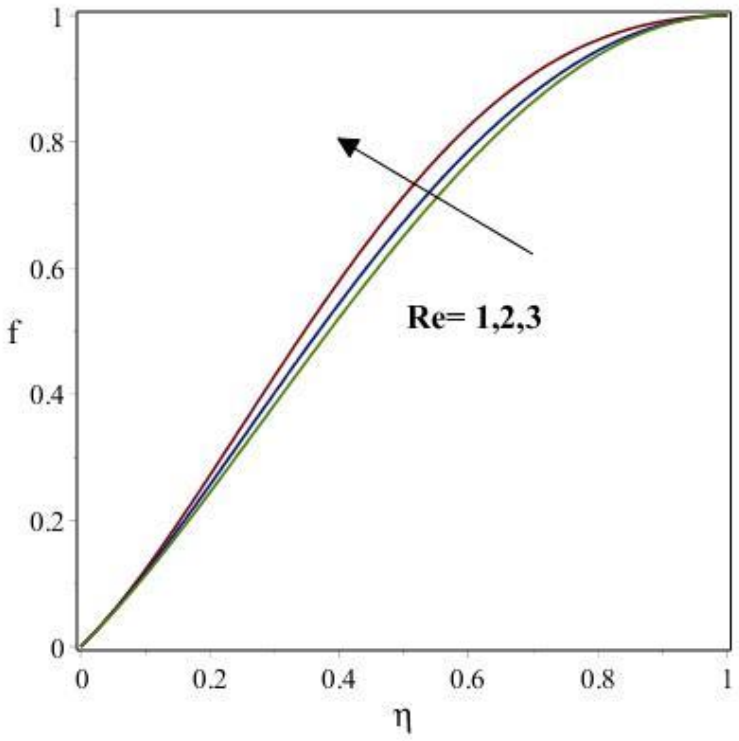

(a)

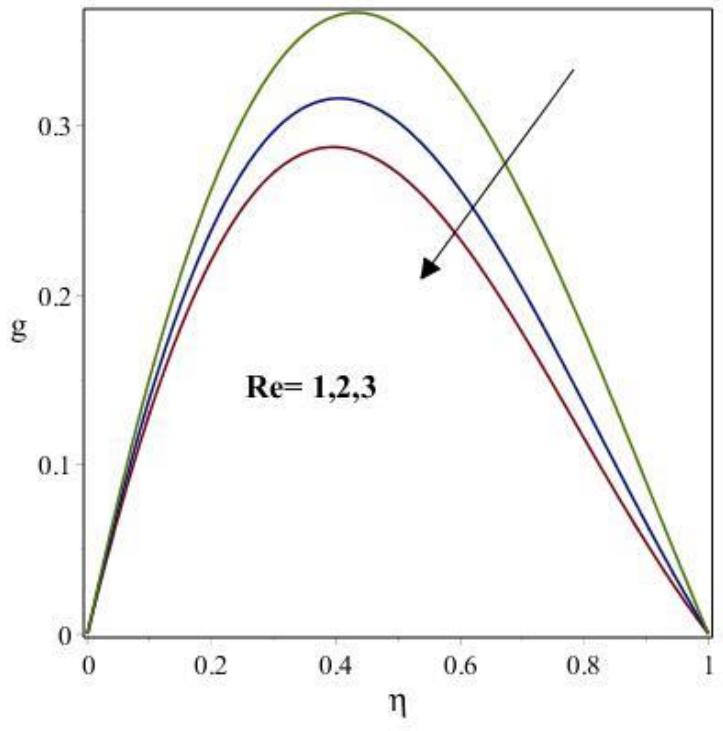

(b)

Figure.(4.3).Variation of Reynold number with velocity profile (a) $f(\eta)$ and (b) $g\ (\eta)$.

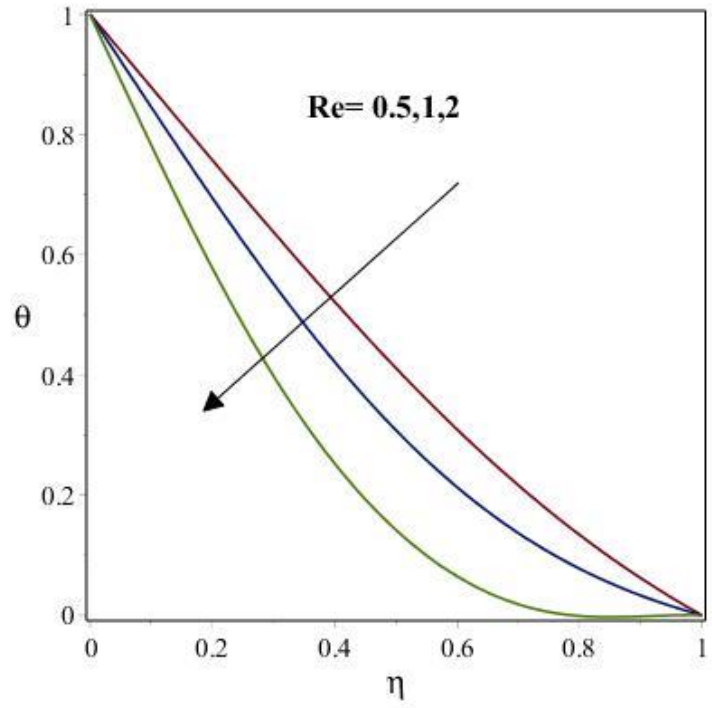

(a)

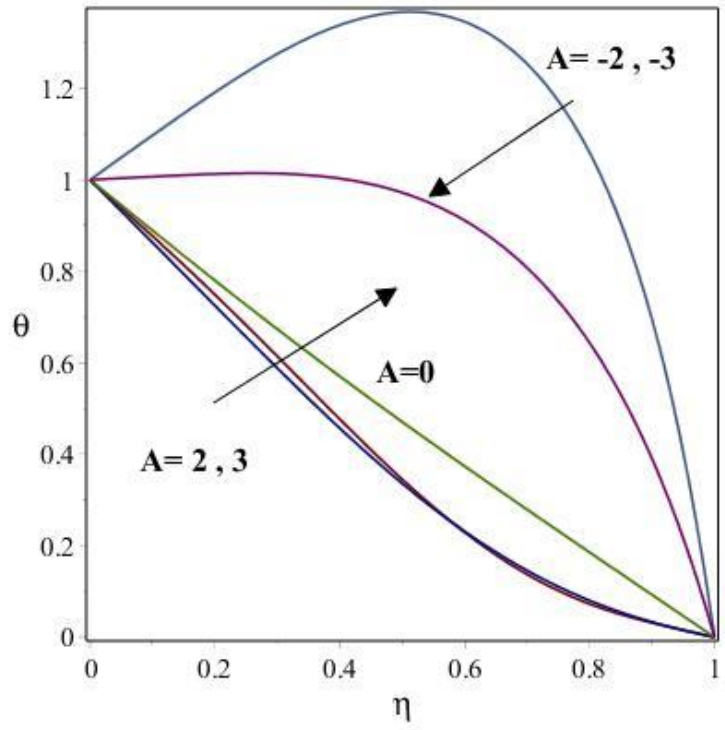

(b)

Figure. (4.4) Influence of (a) *A* and (b) *Re* on the temperature profile..

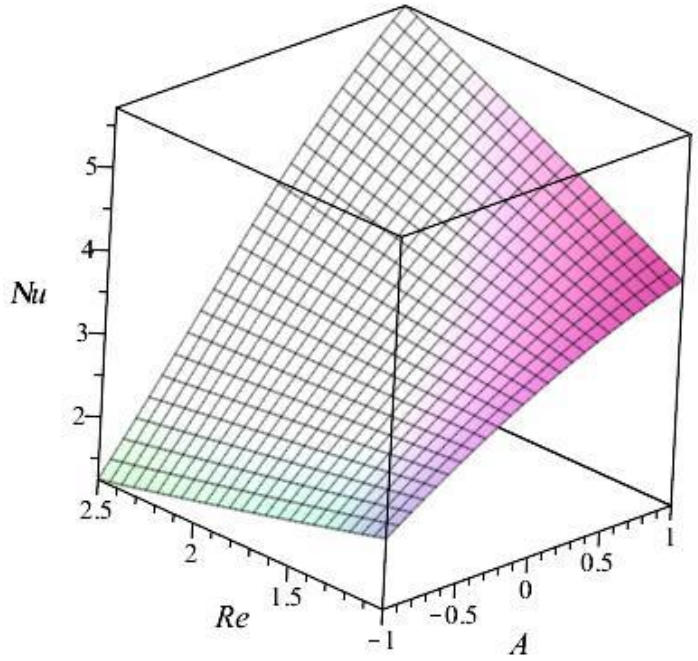

(a)

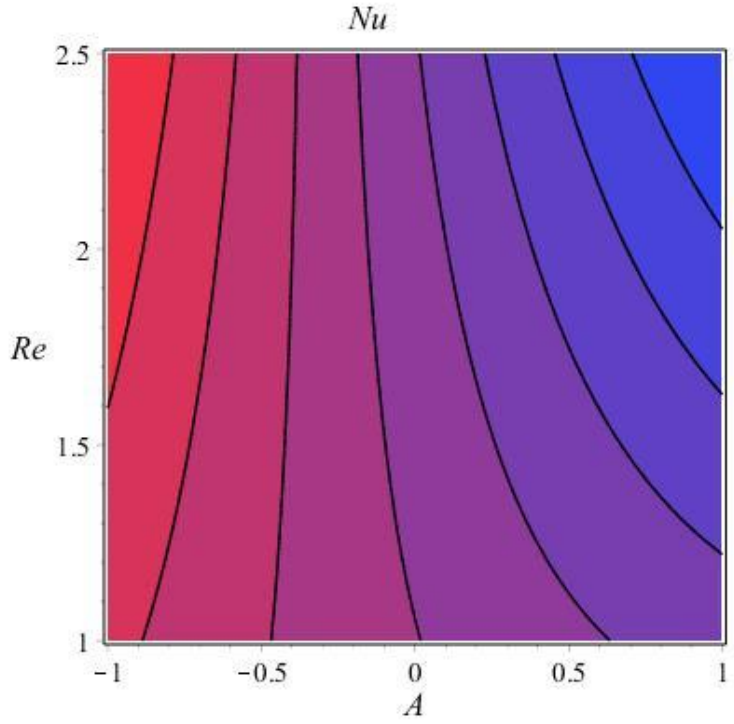

(b)

Figure. (4.5). Variation of (a) *A* and (b) Reynolds number with Nusselt number.

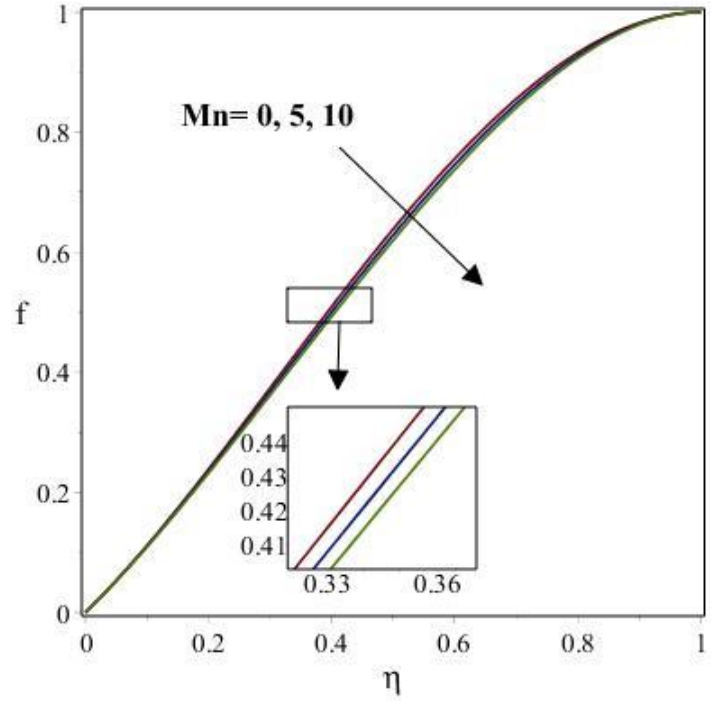

(a)

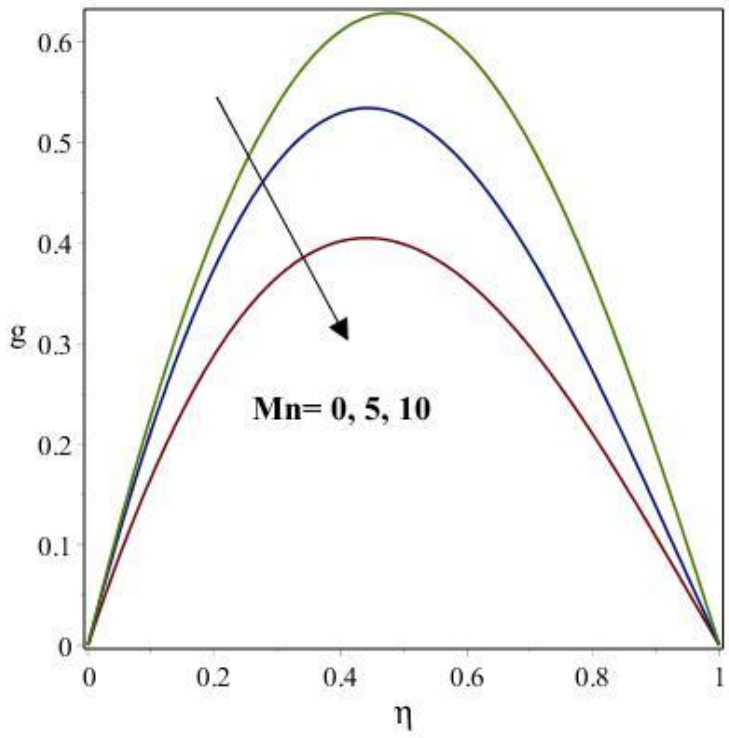

(b)

Figure.(4.6). Variation of magnatic parameter with velocity profile (a) $f(\eta)$ and (b) $g(\eta)$.

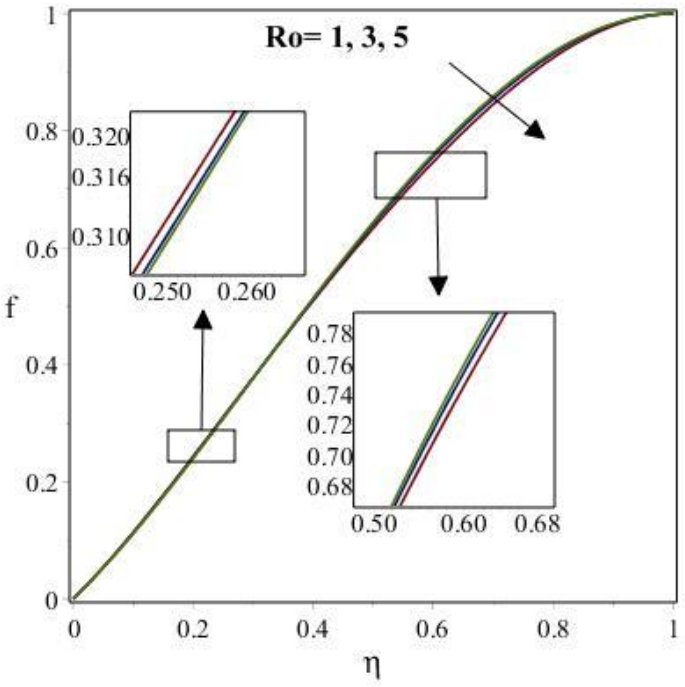

(a)

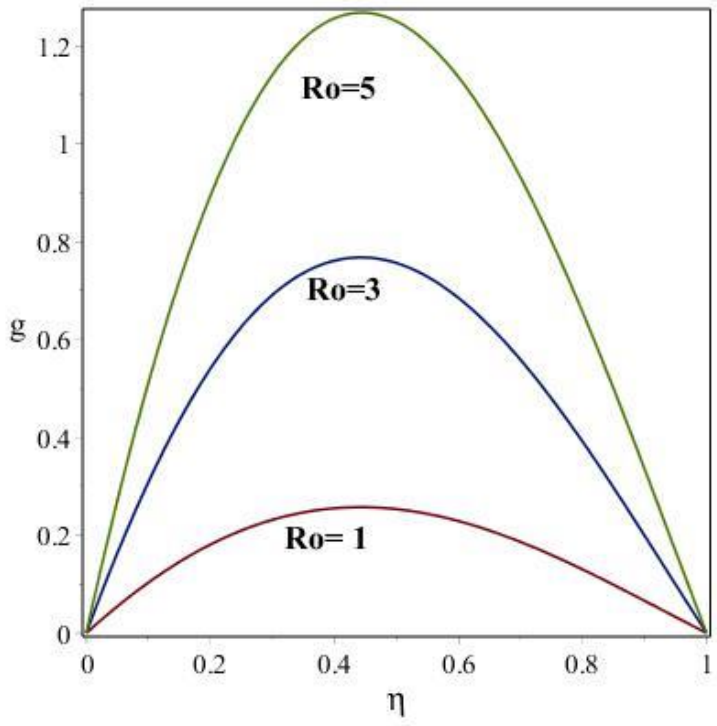

(b)

Figure.(4.7). Variation of *Ro* with velocity profile (a) $f(\eta)$ and (b) $g(\eta)$.

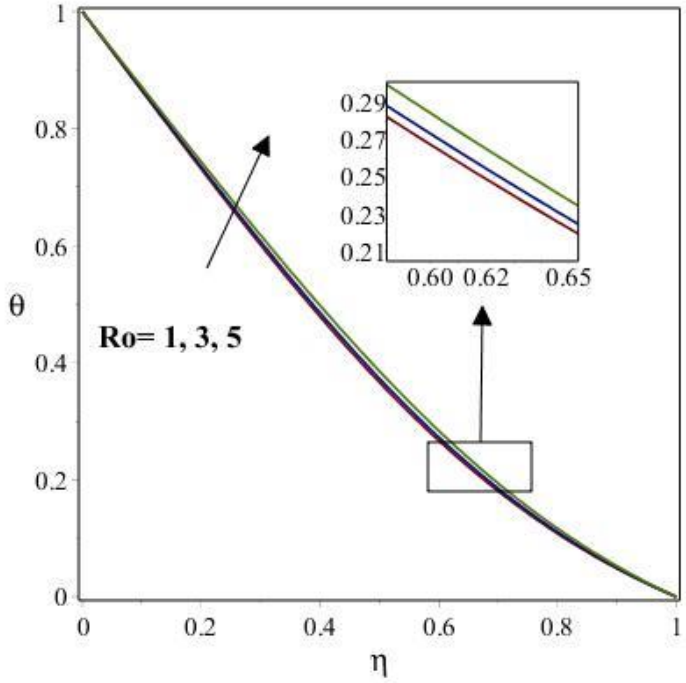

(a)

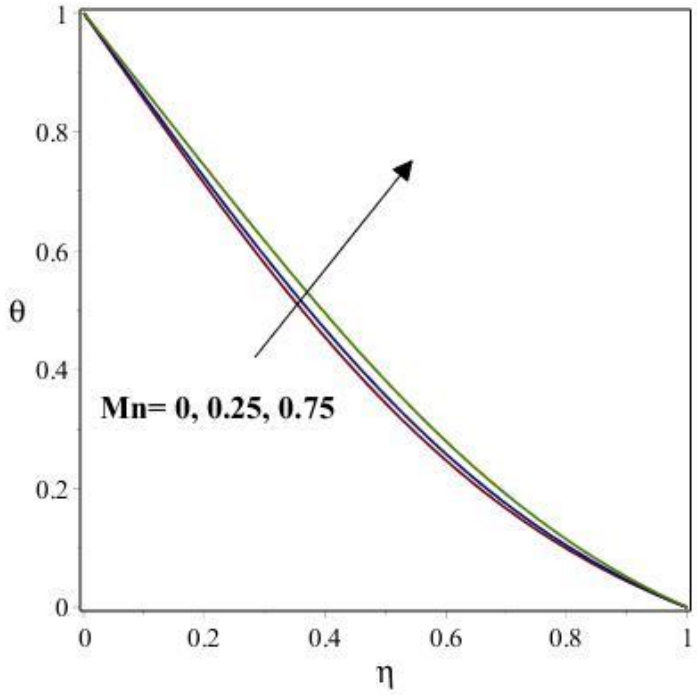

(b)

Figure. (4.8). Influence of (a) rotation and (b) magnetic parameters on the temperature profile.

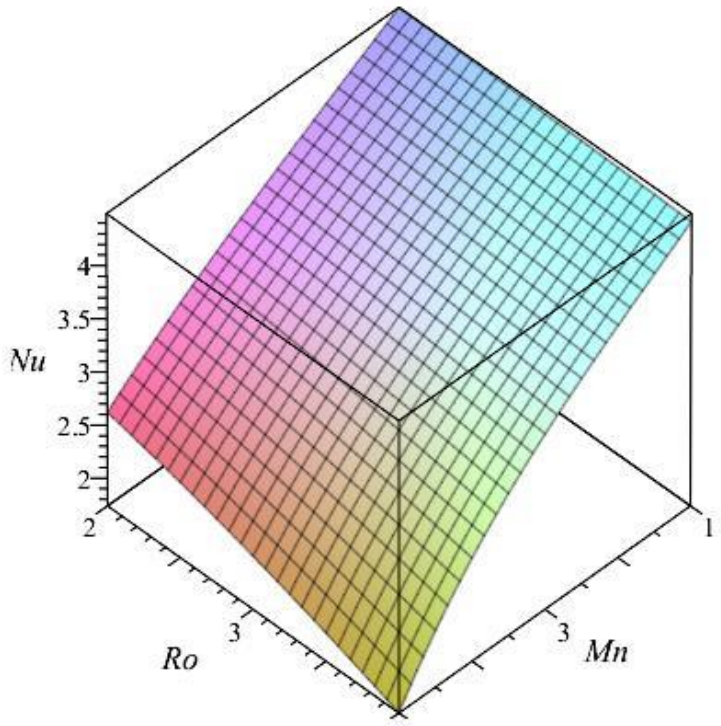

(a)

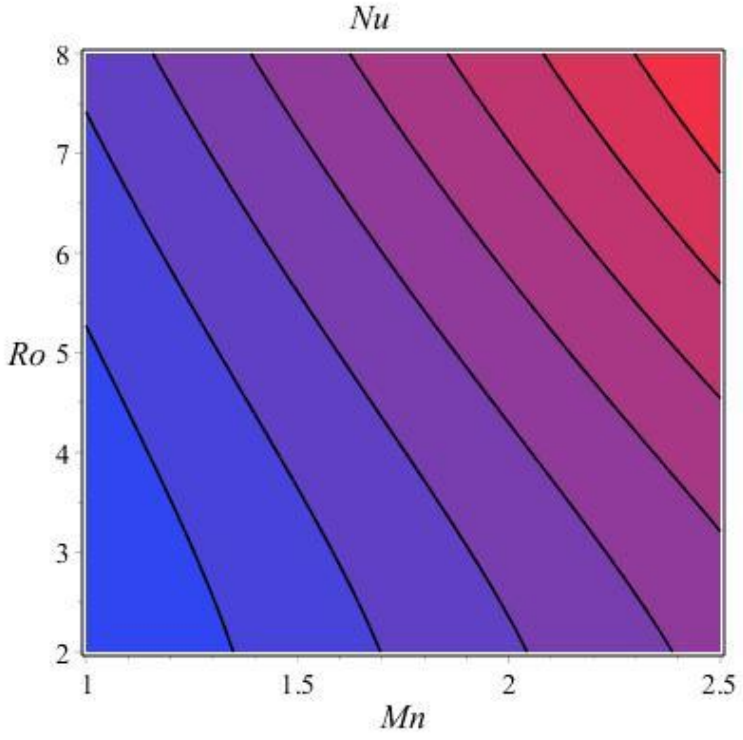

(b)

Figure. (4.9). Influence of (a) magnetic and (b) rotation parameters on the Nusselt number.

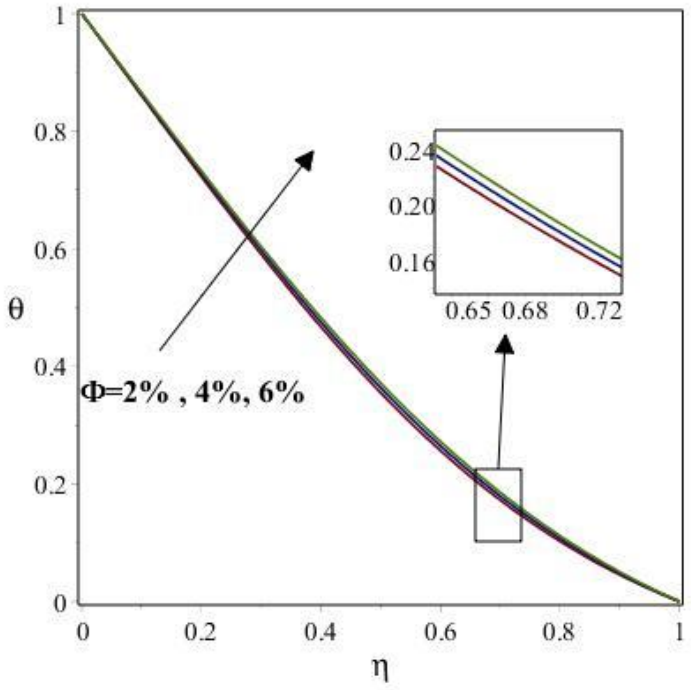

(a)

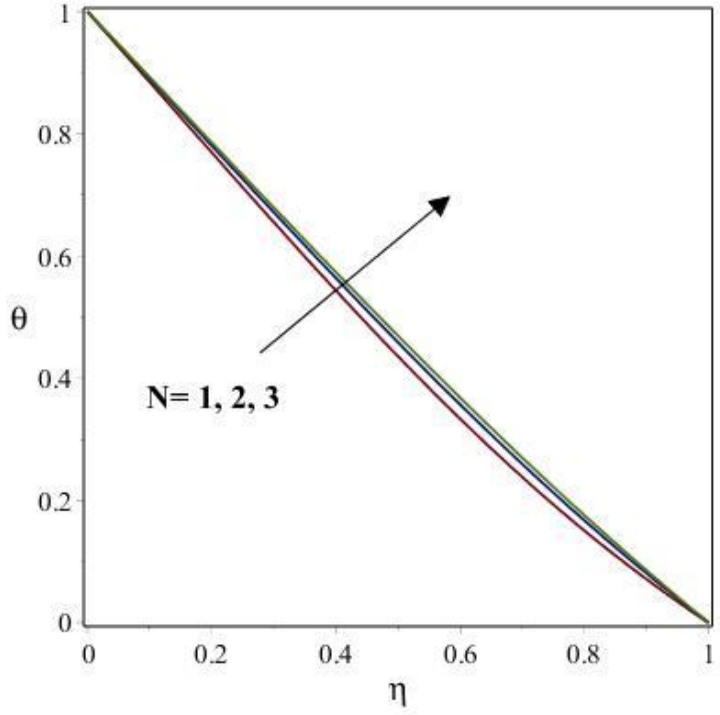

(b)

Figure. (4.10). Effect of (a) N and (b) ϕ on the temperature profile.

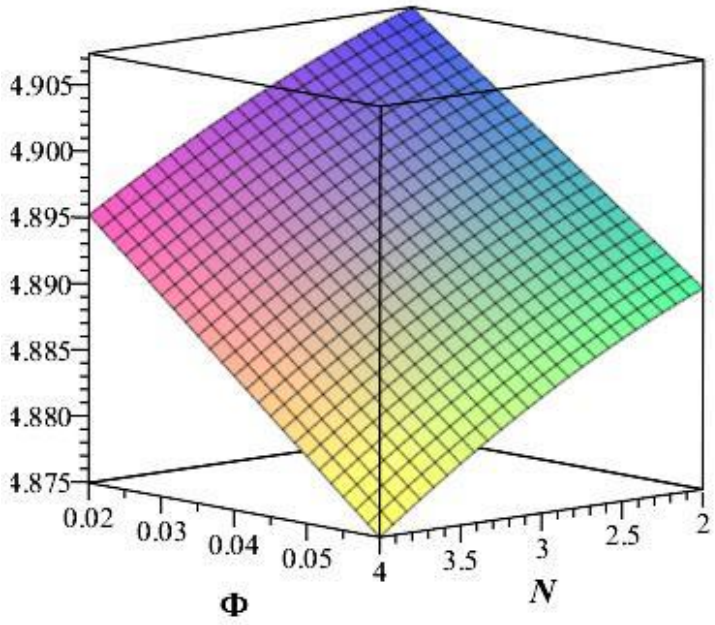

(a)

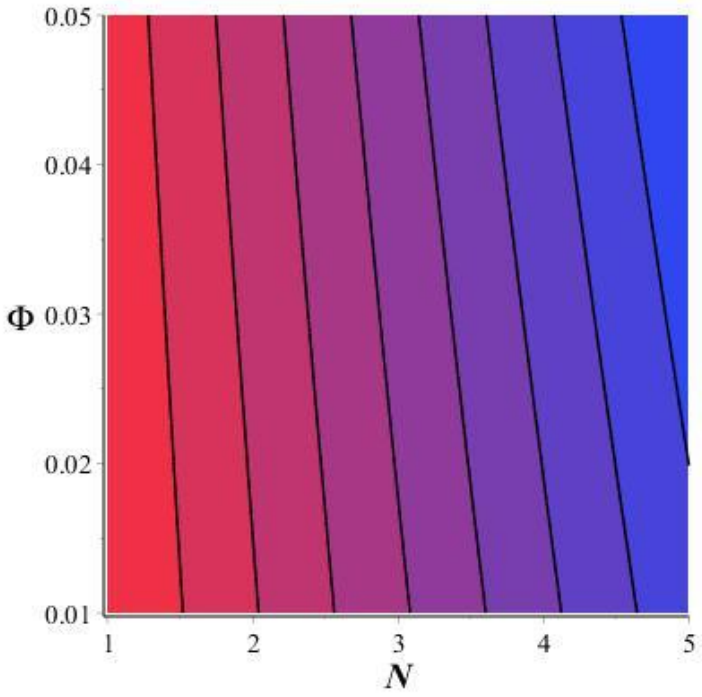

(b)

Figure. (4.11). Variation of (a) radiation parameter and (b) volume fraction with Nusselt number.

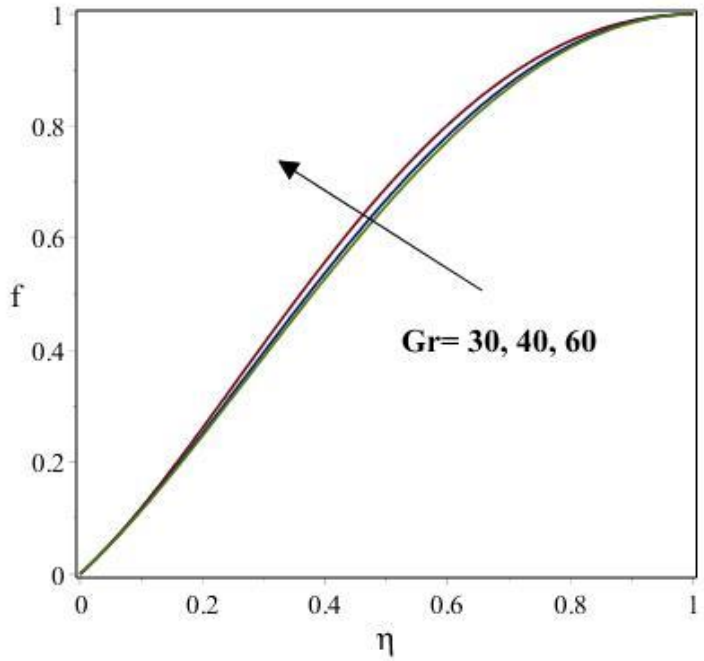

(a)

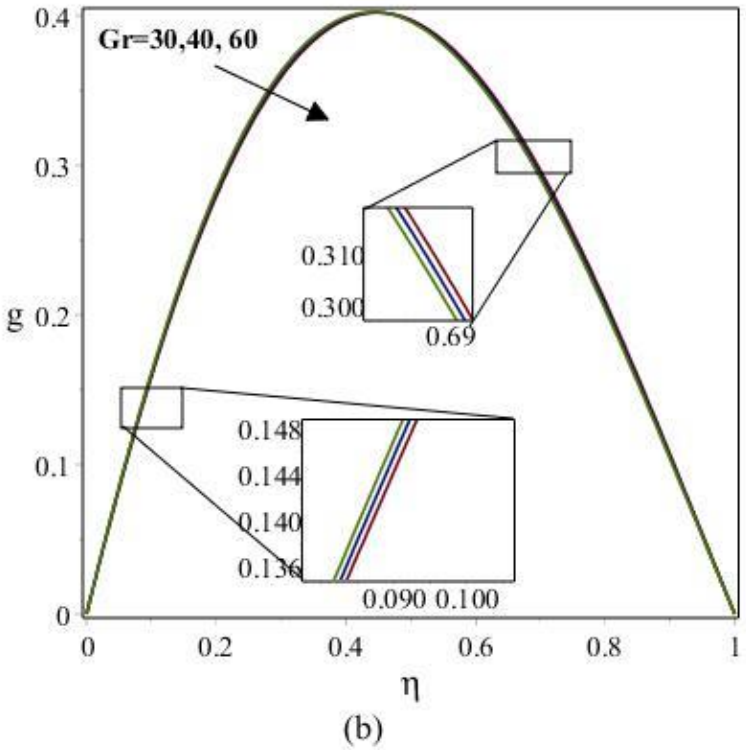

(b)

Figure. (4.12). variation of Grashaf number with velocity profile (a) $f(\eta)$ and (b) $g(\eta)$.

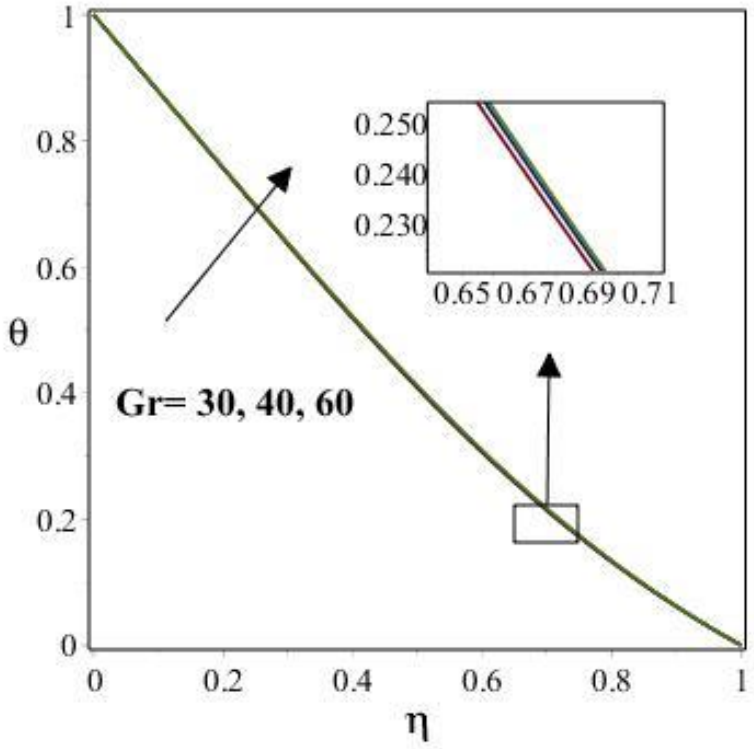

Figure.(4.13). variation of Grashaf number with temperature profile.

Chapter 5

Conclusion

Hybrid nanofluid flow in a vertical channel and heat transfer on a stretchable surface between two plates are examined. The nonlinear PDE's are converted in to ODE's and then solve by using (DRA) Approach. Physical parameter are graphically determined. The obtaining results of this study are

- $A>0$ shows injection and $A<0$ shows suction with wall.
- Both velocities $f(\eta)$ and $g(\eta)$ in x and z-direction increases with increasing injection parameter but suction parameter shows converse behavior.
- Temperature shows decreasing behavior with injection parameter.
- Velocity $f(\eta)$ in x-direction increases with increasing Reynolds number.
- Velocity $g(\eta)$ in z-direction decreases with increasing Reynolds number.
- Nusselt number goes up with raising injection parameter and Reynolds number and also increase for low value of suction parameter.
- Both velocities $f(\eta)$ and $g(\eta)$ in x and z-direction decreasing with increasing magnetic parameter.
- Magnetic and rotation parameter have direct relation with temperature profile.
- Velocity profile $f(\eta)$ clearly goes up and $g(\eta)$ diminish with ascending Rotation parameter.
- Nusselt number diminish with increasing *Mn* and *Ro.*
- With Grashaf number velocity increases in x-direction and decreases in z-direction.
- Temperature profile also increases with Grashaf number.

Bibliography

[1]. S.Choi, Enhancing thermal conductivity of fluids with nanoparticles in developments and applications of non-Newtonian flows: D.A.Siginer, H.P. Wang (Eds.), ASME, 66, 1995, pp.99-105.

[2]. Das, S.K. Putra, N. Thiesen, P. and Roetzel, W. (2003). Temperature Dependence of thermal conductivity Enhancement for Nanofluid. Journal of heat transfer, 125(4), 576.

[3]. Mustafa, T. Hayat, I. Pop, S. Asghare, S.Obaidat, Staganation-point flow of nanofluid towards a stretching sheet,Int. j. Heat Mass Transfer, 54(2011)5588-5594.

[4]. Mustafa, S. Hina, A. Alsaedi, Influence of wall properties on the peristaltic flow of nanofluid: analytic and numerical solutions, Int. J. Heat Mass Transfer 55 (2012) 4871-4877.

[5]. Sheikholeslami, M. Gorji-Bandpy, D.D. Ganji, S. Soleimani, S.M. Seyyedi, Natural convections of nanofluid in an enclosure between a circular and a sinusoidal cylinder in the presence of magnetic field, Int. Commun. Heat Mass Transfer 39 (2012) 1435-1443.

[6]. Soleimani, M. Sheikholeslami, D.D.Ganji, M. Gorji. M. Gorji-Bandpay, Natural convection heat transfer in a nanofluid semi-annulus enclosure, Int. Commun. Heat Mass Transfer 39(2012) 565-574.

[7]. Sheikholeslami, M. Gorji-Bandpy, D.D. Ganji, Magnetic field effects on a natural convection around a horizontal circular inside a square enclosure filled with nanofluid, Int. Commun. Heat Mass Transfer 39 (2012) 978-986.

[8]. Sheikholeslami, M. Gorji-Bandpy, I. Pop, S.Soleimani, Numerical study of a natural convection between a circular enclosure and a sinusoidal cylinder using control volume based finite element method, Int. J. Thermal Sci. 72(2013)147-158.

[9]. Sheikholeslami, M. Gorji-Bandpy, S.M. Seyyedi, D.D. Ganji, H.B. Rokni, S.Soleimani, Application of LBM in simulation of natural convection in a nanofluid filled square cavity with curve boundaries, Powder Tech. 247(2013) 87-94.

[10]. Nadeem, R. Mehmood, N.S. Akbar, Nanoparticle analysis for non-orthogonal stagnation point flow of a third order fluid towards a stretching surface J. Comput. Theor. Nanosci. 10(2013) 2737-2747.

[11]. Alfven. H.L: Existence of electromagnetic hydrodynamic wave. Nature 150. 1942, 405-406.

[12]. Hartman, J. Lazarus, J, Hd-Dynamics II, Theory of Laminar flow Electrically conductive liquids in homogenous magnetic field, 15(7), 1947.

[13]. Rossow, V.J.: On the flow of electrically conducting fluids over a flat plate in the presence of a transverse magnetic field, NASA report No. 1358 (1958).

[14]. M. Mustafa, T. Hayat, and S. Obaidat, "On heat and mass transfer in the unsteady squeezing flow between parallel plates," Meccanica **47**, 1581–1589 (2012).

[15]. M. Alizadeh, A. S. Dogonchi, and D. D. Ganji, "Micropolar nanofluid flow and heat transfer between penetrable walls in the presence of thermal radiation and magnetic field," Case Stud. Therm. Eng. **12**, 319–332 (2018).

[16]. R. Ellahi, Appl. Math. Model. 37 (3) (2013) 1451-1467.

[17]. M. Sheikholeslami, H. R. Ashorynejad, G. Domairry, and I. Hashim, "Flow and heat transfer of Cu-water nanofluid between a stretching sheet and a porous surface in a rotating system," J. Appl. Math. (2012).

[18]. Buongiorno, J. (2006), "Convection transport in nanofluid", ASME Heat Transfer, 128, pp. 240-250.

[19]. Tiwari, R.K. and M.K. (2007), "Heat transfer augmentation in a two-sided lid driven differently heated square cavity utilizing nanofluid", Int.J. Heat Transfer, 50, pp. 2002-2018.

[20]. Ebaid, A., Aly, E.H. and Abdelazem, N.Y. (2014), "Analytical and numerical investigation for the flow and heat transfer of nanofluids over a stretching sheet with partial slip boundary condition", J.Appl.Math. Inf. Sci., 8(4), pp. 1639.

[21]. Vajravelu, K., Prasad, K.V., Lee, J., Lee, C., Pop, I. and V.Gorder, R.A. (2011), "Convection heat transfer in the flow of viscous Ag-Water and Cu-water nanofluids over a stretching surface", Int.J. Therm.Sci. 50, pp. 843-851.

[22]. Hamada, M.A.A., Pop, I. and Md.Ismail, A.I. (2011), "Magnetic field effects on free convection flow of a nanofluid past a vertical semi-infinite flat plate", Nonlinear Analysis: Real World Applications, 12, pp.1338-1346.

[23]. Rana, P. and Bhargava, R. (2011), "Numerical study of heat transfer enhancement in mixed convection flow along a vertical plate with heat source/sink utilizing nanofluid", Commun, Nonlinear Sci. Numer. Simulat. 16, pp.4318-4334.

[24]. Nadeem, S., UI Haq, R. and H.khan, Z. (2014), "Heat transfer analysis of water-based nanofluid over an exponentially stretching sheet", Alexandria Engineering Journal, 53, pp.219-224.

[25]. Bachok, N., Ishak, A., Nazar, R. and Pop, I. (2010), "Flow and heat transfer at a general three-dimensional stagnation point in a nanofluid", Physica B, 405, pp. 4914-4918.
[26]. Hatami, M., Nouri, R, and Ganji, D.D. (2013), "Forced convection analysis for MHD Al_2O_3-water nanofluid flow over a horizontal plate", Journal of Molecular Liquids, 187, pp. 294-301.
[27]. Sheikholeslami, M., Hatami, M. and D.D. Ganji. (2014), "Nanofluid flow and heat transfer in a rotating system in the presence of a magnetic field", Journal of Molecular Liquids, 190, pp. 112-120.
[28]. Sheikholeslami, M., Gorji-Bandpy, M. and Solemani, S. (2103), "Two phase simulation of nanofluid flow and heat transfer using heatline analysis", Int. Comm. Heat and Mass Transfer, 2013.07.006.

[29]. Das, K. (2012), "Slip flow and convection heat transfer of nanofluid over a permeable stretching surface", Computer and fluids, 64, pp.34-42.

[30]. Bachok, N., Ishak, A., Nazar, R. and Pop, I. (2010), "Flow and heat transfer at a general three-dimensional stagnation point in a nanofluid", Physica B, 405, pp. 4914-4918.

[31]. Sheikholeslami, M., Gorji-Bandpy, M. and Solemani, S. (2103), "Two phase simulation of nanofluid flow and heat transfer using heatline analysis", Int. Comm. Heat and Mass Transfer, 2013.07.006.

[32]. A. J. Chamkha, I. V. Miroshnichenko, and M. A. Sheremet, "Numerical Analysis of unsteady conjugate natural convection of hybrid water-based Nanofluid in a semicircular cavity," J. Therm. Sci. Eng. Appl. **9**, 041004 (2017).

[33]. R. S. R. Gorla, S. Siddiqa, M. A. Mansour, A. M. Rashad, and T. Salah, "Heat source/sink effects on a hybrid nanofluid-filled porous cavity,"J. Thermophys Heat Transfer (2017).
[34]. T. Tayebi and A. J. Chamkha, "Free convection enhancement in an annulus between horizontal confocal elliptical cylinders using hybrid nanofluids," Numer. Heat Transfer, Part A **70**, 1141–1156 (2016).
[35]. Liao, S. J., 2003, Beyond Perturbation: Introduction to Homotopy Analysis Method, CRC, and Boca Raton, FL.